Arabian Journal of Chemistry (2020) 13, 9145–9165

King Saud University

Arabian Journal of Chemistry

www.ksu.edu.sa
www.sciencedirect.com

ORIGINAL ARTICLE

One-pot multicomponent synthesis of novel 3, 4-dihydro-3-methyl-2(1*H*)-quinazolinone derivatives and their biological evaluation as potential antioxidants, enzyme inhibitors, antimicrobials, cytotoxic and anti-inflammatory agents

Samra Farooq [1], Aqsa Mazhar [1], Ihsan-Ul-Haq [1], Naseem Ullah [1,*]

Department of Pharmacy, Faculty of Biological Sciences, Quaid-I-Azam University, Islamabad 45320, Pakistan

Received 7 September 2020; accepted 28 October 2020
Available online 6 November 2020

KEYWORDS

3, 4-Dihydro-3-methyl-2 (1*H*)-quinazolinone;
Antioxidant;
Enzyme inhibition;
Antimicrobial;
MTT assay;
Anti-inflammatory assay

Abstract A series of novel 3, 4-dihydro-3-methyl-2(1*H*)-quinazolinone derivatives with substituted amine moieties (**1**–**13**) and substituted aldehyde (**S**) were designed and synthesized by a reflux condensation reaction in the presence of an acid catalyst to get N-Mannich bases. Mannich bases were evaluated pharmacologically for their antioxidant, α-amylase enzyme inhibition, antimicrobial, cell cytotoxicity and anti-inflammatory activities. Most of the compounds exhibited potent activities against these bioassays. Among them, **SH1** and **SH13** showed potent antioxidant activity against DPPH free radical at IC_{50} of 9.94 ± 0.16 μg/mL and 11.68 ± 0.32 μg/mL, respectively. **SH7**, **SH10** and **SH13** showed significant results in TAC and TRP antioxidant assays, comparable to that of ascorbic acid. **SH2** and **SH3** showed potent activity in inhibiting α-amylase enzyme at IC_{50} of 10. 17 ± 0.23 μg/mL and 9.48 ± 0.17 μg/mL, respectively, when compared with acarbose (13.52 ± 0. 19 μg/mL). **SH7** was the most active against gram-positive and gram-negative bacterial strains, **SH13** being the most potent against *P. aeruginosa* by inhibiting its growth up to 80% (MIC = 11.11 μg/mL). **SH4**, **SH5** and **SH6** exhibited significant activity against some fungal strains. Among the thirteen synthesized compounds (**SH1-SH13**), four were screened out based on the results of brine

* Corresponding author.
E-mail addresses: samrafarooq@bs.qau.edu.pk (S. Farooq), aqsamazhar1947@gmail.com (A. Mazhar), ihaq@qau.edu.pk (Ihsan-Ul-Haq), nullah@qau.edu.pk (N. Ullah).
[1] All authors contributed equally to this work.
Peer review under responsibility of King Saud University.

Production and hosting by Elsevier

https://doi.org/10.1016/j.arabjc.2020.10.039
1878-5352 © 2020 The Authors. Published by Elsevier B.V. on behalf of King Saud University.
This is an open access article under the CC BY-NC-ND license (http://creativecommons.org/licenses/by-nc-nd/4.0/).

shrimp lethality assay (LD_{50}) and cell cytotoxicity assay (IC_{50}), to determine their anti-cancer potential against Hep-G2 cells. The study was conducted for 24, 48, and 72 h. **SH12** showed potent results at IC_{50} of 6.48 μM at 72 h when compared with cisplatin (2.56 μM). An *in vitro* nitric oxide (NO) assay was performed to shortlist compounds for *in vivo* anti-inflammatory assay. Among shortlisted compounds, **SH13** exhibited potent anti-inflammatory activity by decreasing the paw thickness to the maximum compared to the standard, acetylsalicylic acid (ASA).

© 2020 The Authors. Published by Elsevier B.V. on behalf of King Saud University. This is an open access article under the CC BY-NC-ND license (http://creativecommons.org/licenses/by-nc-nd/4.0/).

1. Introduction

Under certain pathophysiological conditions, the body starts to produce free radicals in the form of reactive oxygen species (ROS) and reactive nitrogen species (RNS). These free radicals interact with genomic matter (DNA) causing cell disruption which ultimately leads to uncontrolled cell proliferation (Mistry et al., 2017). These radicals act as oxidants and can donate and accept an electron, which plays a crucial role in the pathogenesis of many diseases such as cancer (Valko et al., 2007). "Oxidative stress" is an imbalance between oxidants and antioxidants in the body, which can lead to the damage nucleic acid, essential proteins and tissues (Lobo et al., 2010). Antioxidants can quench these oxidants and help to modulate the progression of carcinogenesis (Kattappagari et al., 2015).

Enzymes are involved in the catalysis of most important biochemical reactions, therefore enzyme inhibitors play a major role in inhibiting these biochemical pathways to regulate disease control and treatment (Shyma et al., 2015). Controlled monosaccharides absorption and carbohydrates digestion is a useful tool to monitor postprandial blood sugar levels to avoid medical conditions such as diabetes, hyperlipidemia, obesity, heart diseases, etc. Kim, 2004. Commercially available amylase inhibitors have many side effects i.e. diarrhea and flatulence Bekirkan et al., 2015 therefore, researchers are always in search of novel α-amylase inhibitors that have fewer side effects and they maintain blood sugar levels within the acceptable range by delaying the starch breakdown.

Microbial resistance is increasing worldwide owing to a growing number of immuno-compromised patients of HIV infection, organ transplantation and cancer chemotherapy (Bayrak et al., 2009). The poor bioavailability, high risk of toxicity, the incidence of microbial resistance and diagnosis at later stages of the disease are the main causes of treatment failure in many patients (Abrão et al., 2015). So it's the need of the hour to design, discover and synthesize new anti-bacterial and anti-fungal agents (Idhayadhulla et al., 2014). The alarming number of microbial and fungal infections integrated with their arising resistance has been driving researchers to design novel and potent antimicrobial compounds with fewer side effects (Essghaier et al., 2014).

Cancer is a term used for the uncontrolled growth of cells (Raghunandan et al., 2011). Despite recent progress and success in treatment modalities, cancer remains the leading cause of morbidity and mortality all over the world (Hoskin and Ramamoorthy, 2008). The mortality rate of cancer remains the second-highest in the United States in 2016 (Siegel et al., 2016). Besides, the prevalence of cancers of the kidney, breast, liver and prostate, continues to expand every year (Zhang et al., 2010). The discovery and development of new bioactive molecules remain the necessity to combat cancer. Researchers are working on new anticancer approaches that aim at inducing apoptosis in the affected cells, thus minimizing their proliferation (Belluti et al., 2010). Therefore, many organic anticancer agents have been discovered in recent years and are greatly being used in the treatment of cancer (Koca et al., 2013).

Nitric oxide (NO) is a pathophysiological mediator found in the body. It is produced from nitric oxide synthase (NOS) and acts as an antioxidant by scavenging free radical and also interacts with proteins and cyclooxygenase (COX) to modulate physiological functions in the body (Liu et al., 2002). Three isoforms of NOS have been identified, neuronal NOS (nNOS), endothelial NOS (eNOS) and inducible NOS (iNOS) depending upon their function in the body (Moncada, 1997; Murad, 1998). NO produced from eNOS and nNOS are beneficial, whereas, NO produced from iNOS as a result of an injury in response to inflammatory stimuli i.e. cytokines, bacterial endotoxins, etc. is harmful to the body (Grisham et al., 1999). NO plays an important role in inflammation, cancer, aging, diabetes mellitus, etc. therefore, nitric oxide synthase inhibitors play a significant role in regulating the NO level and act as anti-inflammatory agents (Koksal et al., 2017; Lyons, 1995).

Compounds derived from the Mannich reaction are known to have versatile biological properties. They are obtained by condensation reactions of a substrate with an active proton, an aldehyde (mainly formaldehyde) and primary or secondary amines to obtain aminomethylated Mannich bases (Tramontini, 1973; Ashok et al., 2007). Literature survey demonstrates that Mannich bases are known for their diverse properties i.e. analgesics (Rubat et al., 1992), antipyretics (Almirante et al., 1965), antimicrobials (Pandeya et al., 1999), anti-cancer (Holla et al., 2003), antioxidants (Ünver et al., 2016), anti-inflammatory (Sivakumar et al., 2014) and anticonvulsant (Sridhar et al., 2002).

Heterocyclic compounds are versatile and important compounds in medicinal chemistry (Al-Mulla, 2017). Their number is increasing due to their easy manipulation in organic synthetic reactions and facile derivatization (Saleh et al., 2019). Heterocyclic structures possess a condensed ring system (Saini et al., 2013) and exhibit promising and remarkable pharmacological activities (Akram et al., 2017) i.e. antibacterial (Chao et al., 2005; Srinivas et al., 2006; Banday et al., 2010; Saad, 1996; Nanjunda et al., 2006), antifungal (Chen et al., 2007, 2008), anti-allergic (Roy et al., 1997; Tanabe et al., 1997; Trapani et al., 1992; Wade et al., 1979), anti-inflammatory (Burbuliene et al., 2004; Chandra et al., 2010; Akhter et al., 2009; Dewangan et al., 2010; Jayashankar et al., 2009), anti-cancer (Kok et al., 2008; Wang et al., 2006; Jin et al., 2006; Aboraia et al., 2006), antioxidant (Nishiyama et al., 1998, 2003; Taj et al., 2011; Padmaja

et al., 2009), anticonvulsant (Zarghi et al., 2008, 2005; Almasirad et al., 2004) etc. Some examples of promising marketed drugs with heterocyclic ring structures are summarized in Fig. 1.

Quinazoline is considered among the significant nitrogen-containing heterocyclic compounds in medicinal chemistry. The structural motifs have gained much attention in the past few years because of their diverse chemical reactivity, profound medicinal value, and accessibility. Quinazoline has many derivatives with ketone attached to it; referred to as quinazolinones (Ajani et al., 2017). Core structural motifs of the quinazoline ring are depicted in Fig. 2.

Quinazolinone belongs to a class of quinazoline heterocyclic compounds (Shi et al., 2013), possessing numerous biological activities (Asadi et al., 2017). Literature survey reveals that quinazolinone derived analogues are potential anti-cancer (Marzaro et al., 2012), anti-inflammatory (Alaa et al., 2016), antibacterial (Bouley et al., 2015), antifungal (Ryu et al., 2012); antimalarial (Bhattacharjee et al., 2004), antiviral (Wang et al., 2012), antihypertensive (Kumar et al., 2003), anti-tubercular (Raghavendra et al., 2007) agents. Many efforts have been devoted to the separation and purification of naturally occurring quinazolinone alkaloids as well as artificial synthesis of novel quinazolinones with diverse biological properties (Peng et al., 2015). They are present in various drug molecules, such as quinethazone as a diuretic drug and methaqualone as a potential anticonvulsant drug that has been used in clinics (Sharma et al., 2011). More interestingly, an increasing number of quinazolinone derivatives have displayed great potency in the treatment of microbial infections (Shi et al., 2013; Al-Omary et al., 2013) i.e. Febrifugine and isofebrifugine (Mital, 2007). Some promising structures of the quinazolinone ring with their pharmacological activity are summarized in Fig. 3.

The hybridization of functional groups with a biologically active molecule leads to products that have synergistic effects (Kumar et al., 2012). This is an attractive approach now a days to design and synthesize new bioactive compounds. Considering the biological applications of the quinazolinone heterocyclic ring system and our long standing interest in investigating the Mannich bases, in the present work, we used one-pot multicomponent approach to synthesize a series of Mannich bases of quinazolinone moiety. The Mannich products synthesized in the present work have not been reported in the literature to date. The entire synthetic library was subsequently evaluated in biological studies for their *in silico*, antioxidant, α amylase enzyme inhibition, antimicrobial, anti-cancer and anti-inflammatory potential. The newly synthesized compounds were evaluated against hepatocellular carcinoma (HepG2) cell line because there have been studies in the literature citing the cytotoxic nature of the quinazolinone ring and its respective derivatives (Poorirani et al., 2018) but none of the studies was conducted to evaluate the cytotoxic behavior of quinazolinone derivatives against HepG2 cell lines. So, due to this reason HepG2 cell lines were targeted in the current study. Moreover, the comprehensive biological profiling of 3, 4-dihydro-3-methyl-2(1*H*)-quinazolinone derived N-Mannich bases by one-pot multicomponent reac-

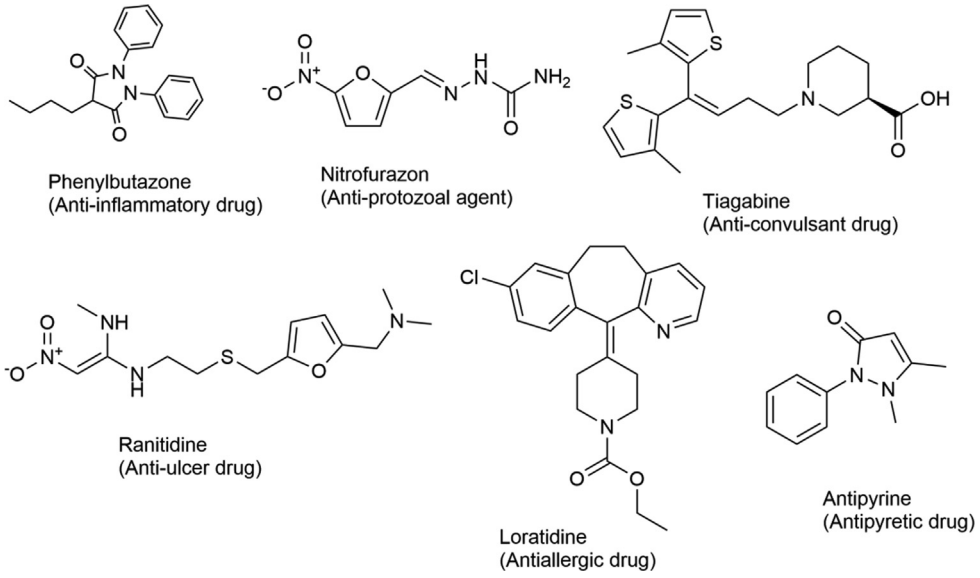

Fig. 1 Selected examples of FDA approved drugs with a heterocyclic ring structure and their pharmacological activities.

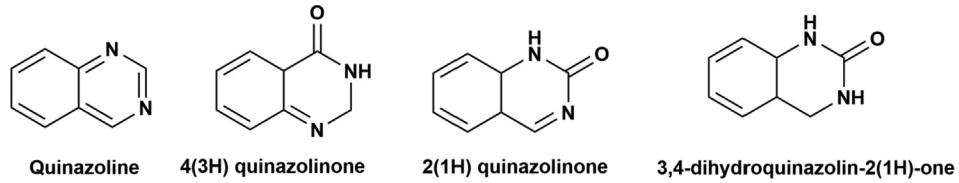

Fig. 2 Structure of quinazoline and its keto derivatives; Quinazolinones.

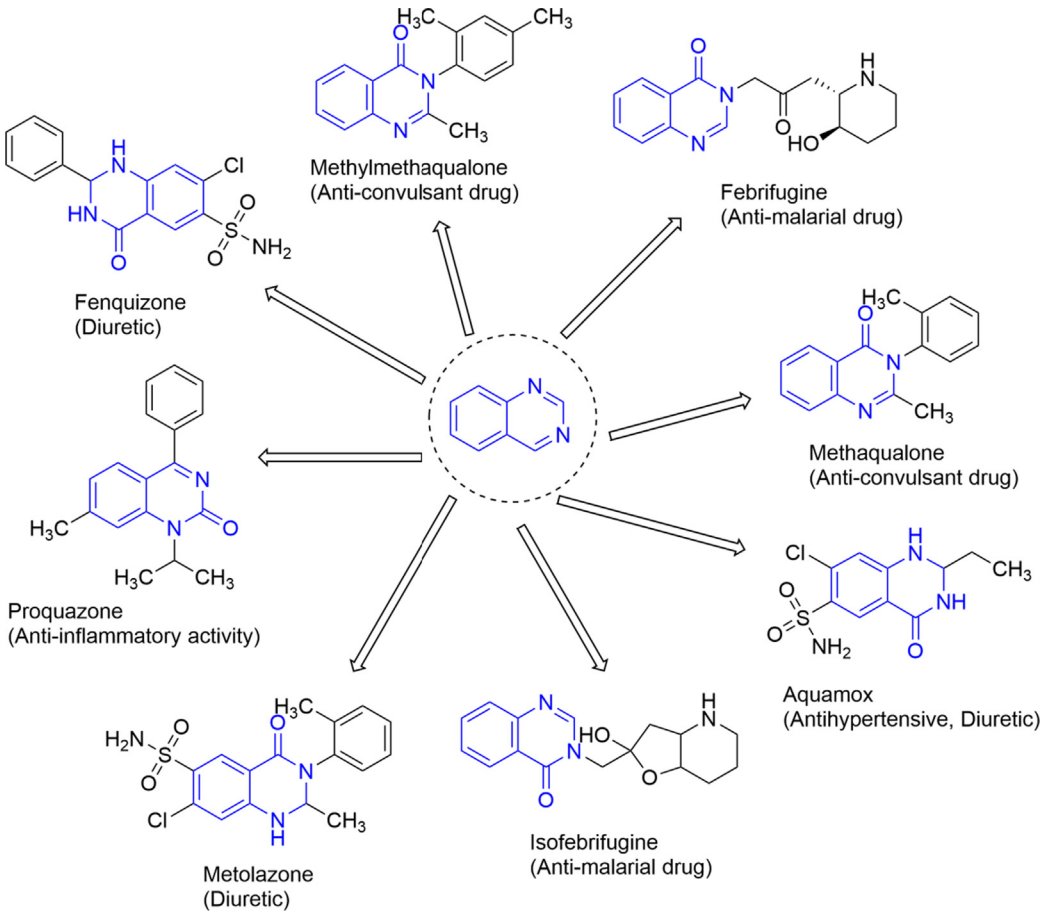

Fig. 3 Selected examples of a quinazolinone ring system containing marketed drugs and their biological activities.

tion (MCR) has not yet been thoroughly probed in the literature before.

2. Results and discussions

2.1. Chemistry

One-pot synthesis is a relatively unique and distinctive approach in organic synthesis (Samu and Janáky, 2017). In organic reactions, one-pot synthesis is generally applied to a multi-step reaction in a single vessel. It has many advantages in terms of saving time, minimal chemical waste, reduction of purification steps, synthetic modifications and bond-forming steps in a single pot (Hayashi, 2016). Because of these benefits, this synthesis is considered to be greener and comes under green chemistry (Sydnes, 2014). One-pot multicomponent reactions (MCRs) are now being extensively used in synthetic organic reactions. For example, tropinone synthesis by one-pot synthesis some 100 years ago by Robinson is a milestone in organic chemistry (Medley and Movassaghi, 2013).

The synthesis of the compounds **SH1-SH13** followed the general pathway outlined in Scheme 1. N-Mannich bases of the quinazolinone moiety (**H**) were synthesized by one-pot multicomponent reflux condensation reaction with substituted amines (**1–13)** and formaldehyde (**S**) placed in a single pot (pressure tube) at 80 °C for ~5–7 h. The product was precipitated and recrystallization was done by ethanol. Flash column chromatography (FCC) was performed to purify the products.

Mannich reaction is a condensation reaction where H_2O is eliminated as a byproduct. It is an example of an S_N2 reaction, where an amine reacts with the carbonyl group of formaldehyde, resulting in an intermediate, which reacts with an acidic proton of the quinazolinone nucleus (Tramontini, 1973). All the quinazolinone derived Mannich bases were obtained in good yield and their structure was confirmed by physical and spectral data. The FTIR spectrum showed stretching bands at around 1663–1748 cm^{-1} region for amidic (C═O) and 1631 cm^{-1} regions for the C═N group. In the ^{1}H NMR spectrum of the newly synthesized compounds, a singlet (s) was observed at δ 4.42-4.44 ppm region which corresponds to the ─CH_2 group, confirming that the Mannich bases were successfully synthesized by a condensation reaction. In the case of **SH4**, **SH8** and **SH13**, a singlet (s) were observed at δ 4.00, 4.80 and 5.02 ppm, respectively. The most downfield chemical shifts observed in the spectrum of these compounds were due to the presence of an electronegative atom (─Br) in **SH8** and ─OH attached to a phenyl ring (acetaminophen substituted) in **SH13**. The aromatic protons of the quinazolinone derivatives were observed as multiplets (m) at the most downfield region of the spectrum around δ 6.74–7.16 ppm. There was a singlet (s) observed between δ 2.00–3.02 ppm for three protons of the ─CH_3 group. In the ^{1}H NMR spectrum of **SH13**, recorded in $CDCl_3$, showed a singlet peak (s) at δ 9.95 ppm

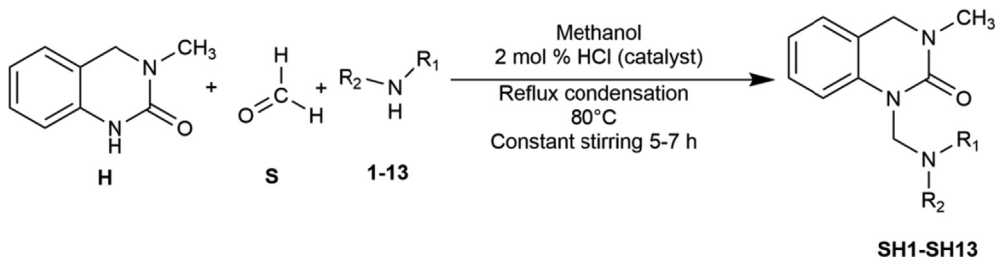

Scheme 1 One-pot multicomponent synthesis of 3, 4-Dihydro-3-methyl-2(1*H*)-quinazolinone derived Mannich bases (**SH1-SH13**).

due to —OH attached to a phenyl group. The solvent peak for $CDCl_3$ was observed at δ 7.26 ppm. Further structural elucidation was confirmed by the ^{13}C NMR spectrum. The most downfield carbons of the quinazolinone moiety were observed near δ 113–155 ppm. The carbon of the methylene imine linkage (N—CH_2—N) was observed near δ 60.34–64.34 ppm for most of the compounds except for **SH7**, **SH8** and **SH11**, which resonated at δ 50.85, 50.81 and 55.55 ppm, respectively. The solvent peaks were observed at δ 77.2 ppm and 39.5 ppm for $CDCl_3$ and DMSO-d_6, respectively. All the other aromatic signals were observed at expected regions. In the mass spectrum of the synthesized compounds, molecular ion peak was observed as (M +) for all the compounds.

2.2. In silico studies

Most of the drugs failed at clinical trials because of their poor absorption, distribution, metabolism and excretion parameters; this is the reason that *in silico* methods are gaining much importance in drug development. ADME-PK has a significant role in measuring the drug likeness and pharmacokinetic parameters of the drug (Ha et al., 2019). The newly synthesized series of synthetic compounds were evaluated for their drug likeness and pharmacokinetic properties. The results of the synthesized compounds are presented in Table 1. All of the newly synthesized compounds passed the Lipinski's screening test and followed the recommended druglike properties.

All the newly synthesized compounds were complying with Lipinski's rule of five. But fulfilling all the parameters does not ensure a compound to be a good orally active drug. There are many examples of marketed drugs that violate Lipinski RO5, but generally, it is acceptable that any drug that violates not more than one parameter can be a good active oral drug (Yehye et al., 2012). It can be predicted that all synthesized compounds are likely to be orally actives as they comply with Lipinski's rule of 5.

2.3. Bioevaluation

2.3.1. Antioxidant assay

2.3.1.1. DPPH free radical scavenging assay (FRSA). The quinazolinone derivatives **SH1-SH13** were evaluated for their free radical scavenging activity (FRSA) at 200, 66.66, 33.33 and 7.41 μg/mL concentration by DPPH radical method using Ascorbic acid and Quercetin as standards. The compounds exhibited significant scavenging activity by discoloring DPPH free radical to stable DPPH molecule. The chemical equation of this conversion is depicted in Fig. 4.

Table 1 Lipinski's rule of five (RO5) for the assessment of pharmacokinetic parameters of the synthesized compounds (SH1 SH13).

Serial #	Compound Name	MW [1] (< 500 Daltons)	HBA [2] (< 10)	HBD [3] (< 5)	Log $P_{o/w}$ (iLOGP) [4] (< 5)	Log $P_{o/w}$ (MLOGP) [5] (< 5)	Lipinski violation
1	**SH1**	259.35	2	0	2.70	2.20	No
2	**SH2**	261.32	3	0	2.51	1.11	No
3	**SH3**	245.32	2	0	2.79	1.94	No
4	**SH4**	275.39	2	0	3.19	2.86	No
5	**SH5**	274.36	3	0	2.72	1.78	No
6	**SH6**	260.33	3	1	2.45	1.11	No
7	**SH7**	343.42	1	0	3.16	3.89	No
8	**SH8**	346.22	1	1	3.22	3.10	No
9	**SH9**	301.77	1	1	2.96	2.98	No
10	**SH10**	309.36	2	0	2.60	2.45	No
11	**SH11**	297.35	2	1	2.91	2.56	No
12	**SH12**	247.34	2	0	2.93	2.35	No
13	**SH13**	325.36	3	1	2.66	1.90	No

[1] MW = Molecular weight
[2] HBA = Hydrogen bond acceptors.
[3] HBD = Hydrogen bond donors
[4] ilog $P_{o/w}$ = octanol-water partition co-efficient.
[5] MLOGP = Moriguchi Log P (octanol-water partition co-efficient).

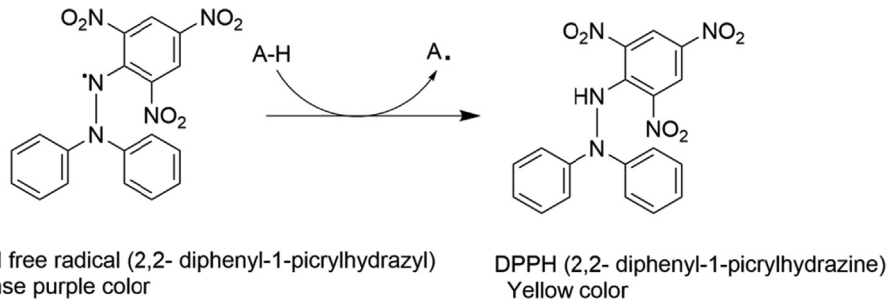

Fig. 4 Oxido-reduction mechanism of DPPH free radical to DPPH stable compound by an antioxidant.

The results of % FRSA of the synthetic compounds and their IC_{50} values are presented in Table 2.

Among the synthesized compounds, **SH1** substituted with piperidine moiety showed the most potent antioxidant activity than both standards at IC_{50} of 9.94 ± 0.16 µg/mL by quenching unstable purple-colored DPPH free radical to stable yellow-colored 2, 2-diphenyl-1-phenylhydrazine molecule. **SH13** has also shown antioxidant activity at IC_{50} value of 11.68 ± 0.32 µg/mL, which was close to the standard, ascorbic acid and lower to that of quercetin, which has IC_{50} values of 11.09 ± 0.06 and 16.56 ± 0.03 µg/mL, respectively. It is reported in the previous studies that compounds substituted with heterocyclic piperidine ring possess scavenging properties against DPPH free radical and are considered to be good antioxidants (Rk et al., 2018; Das and da Silva, 2018). Acetaminophen, an analog of Paracetamol also showed significant antioxidant activity. This is due to the transfer of a proton from the phenolic —OH to DPPH free radical (Alisi et al., 2012). Compounds having —OH and $—OCH_3$ groups in the benzene ring possess stronger antioxidant activities by scavenging DPPH free radical (Rakesh et al., 2015). All other compounds showed moderate to good antioxidant activity.

2.3.1.2. Total antioxidant capacity (TAC) and Total reducing potential (TRP) assay. The synthetic compounds were further evaluated *in vitro* for their antioxidant potential by using the phosphomolybdenum based antioxidant assay. The highest TAC was exhibited by **SH7**, followed by **SH 10** and **SH5** at 154.44 ± 1.9, 88.66 ± 1.71 and 84.49 ± 2.1 µg/AAE, respectively. The results are summarized in Fig. 5. Ascorbic acid standard curve was plotted and the regression equation was used for TAC and TRP estimations (Fig. 6).

The formation of a green-colored phosphomolybdenum complex was analyzed by the spectrophotometric method (Prieto et al., 1999). The least antioxidant activity was shown by **SH1** and **SH6**. All other compounds exhibited moderate activity.

A TRP assay was performed to determine the reducing power of the compounds. Only **SH12** and **SH13** showed antioxidant activity in TRP assay. Reducing power of any compound is dependent on the groups which were substituted in the molecule. The presence of the phenol ring in the compound plays an important role to act as an electron donor ultimately increasing the reducing power of the compound (Cetin and Geçibesler, 2015). Moreover, —OH group attached to a

Table 2 % Free Radical Scavenging Assay of synthetic compounds at different concentrations and their IC_{50} values.

Serial #	Compounds	% DPPH free radical scavenging activity (FRSA) at different concentrations				IC_{50} µg/mL[1]
		200 µg/mL	66.66 µg/mL	22.22 µg/mL	7.41 µg/mL	
1	**SH1**	90.31 ± 0.31	75.37 ± 0.18	51.21 ± 0.16	42.47 ± 0.27	9.94 ± 0.16
2	**SH2**	21.21 ± 0.28	12.21 ± 0.31	9.91 ± 0.11	2.98 ± 0.12	551.01 ± 0.34
3	**SH3**	32.68 ± 0.22	21.11 ± 0.27	11.34 ± 0.21	8.76 ± 0.11	334.86 ± 0.23
4	**SH4**	34.45 ± 0.19	18.71 ± 18	7.89 ± 0.10	2.42 ± 0.21	290.77 ± 0.31
5	**SH5**	45.28 ± 0.24	38.27 ± 0.21	20.91 ± 0.17	17.89 ± 0.34	216.50 ± 0.18
6	**SH6**	47.81 ± 0.26	33.31 ± 0.23	21.89 ± 0.16	14.24 ± 0.27	203.49 ± 0.24
7	**SH7**	10.71 ± 0.17	4.76 ± 0.14	2.98 ± 0.14	0.89 ± 0.29	916.01 ± 0.41
8	**SH8**	50.41 ± 0.33	37.71 ± 0.18	24.21 ± 0.21	12.24 ± 0.33	182.84 ± 0.27
9	**SH9**	25.11 ± 0.21	18.91 ± 0.42	12.24 ± 0.11	9.89 ± 0.16	520.21 ± 0.31
10	**SH10**	54.03 ± 0.11	40.81 ± 0.32	32.42 ± 0.21	21.61 ± 0.19	161.17 ± 0.18
11	**SH11**	36.33 ± 0.28	29.23 ± 0.18	20.91 ± 0.14	15.45 ± 0.14	325.80 ± 0.19
12	**SH12**	44.28 ± 0.18	37.39 ± 0.11	29.91 ± 0.19	26.64 ± 0.22	254.47 ± 0.52
13	**SH13**	89.73 ±	70.91 ± 0.22	53.34 ± 0.18	42.24 ± 0.38	11.68 ± 0.32
14	**Blank**	0	0	0	0	–
15	**Ascorbic Acid**	89.01 ± 0.18	68.81 ± 0.17	52.23 ± 0.31	44.71 ± 0.23	11.09 ± 0.06
16	**Quercetin**	81.43 ± 0.21	69.81 ± 0.17	58.31 ± 0.28	42.34 ± 0.36	16.56 ± 0.03

[1] IC_{50} is the concentration of the synthetic compounds that is required to scavenge 50% of the DPPH molecule; values are described as Mean ± SEM (standard error of the mean, $n = 3$).

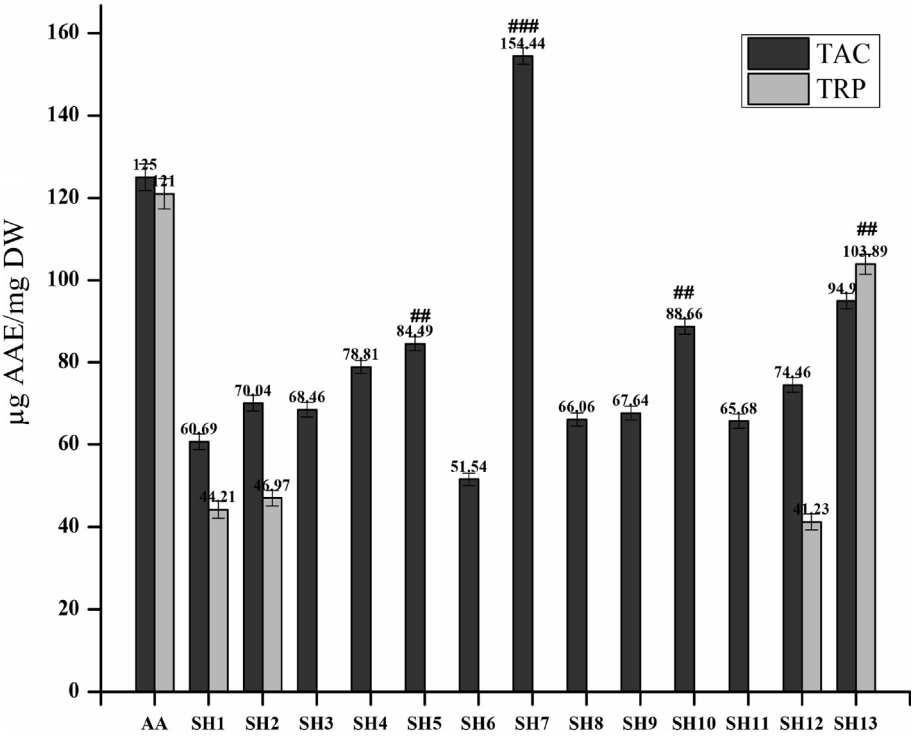

Fig. 5 Total antioxidant capacity (TAC) and Total reducing power (TRP) assay values of the synthetic compounds compare with the standard i.e. ascorbic acid (AA). Values are expressed as ascorbic acid equivalent (AAE). ###/## indicates $p < 0.01$ and $p < 0.05$, respectively.

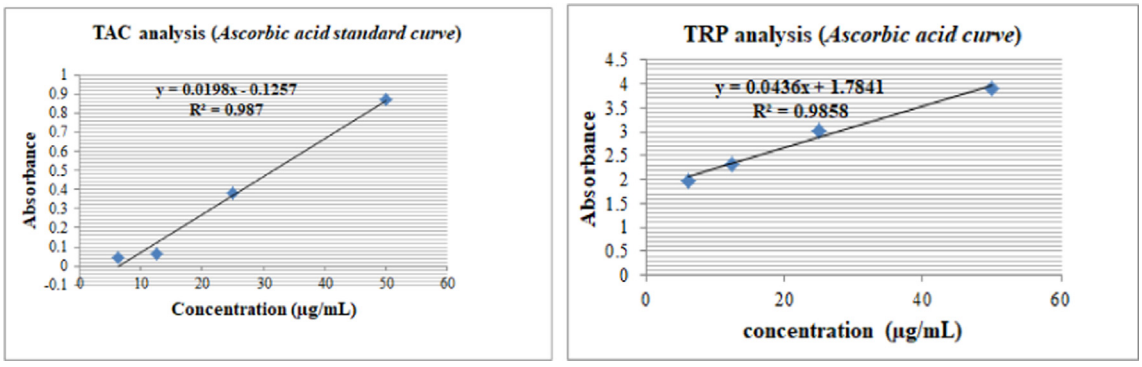

Fig. 6 Ascorbic acid standard curve ($R^2 = 0.987$) for TAC assay and ($R^2 = 0.9858$) for TRP estimations.

benzene ring, **SH10** and **SH13,** is responsible for antioxidant potential (Rakesh et al., 2015).

Some of the synthetic compounds that have shown good antioxidant activity in %FRSA assay did not show any significant activity in TAC and TRP assay i.e. **SH1**. This is because antioxidant compounds act through different chemical pathways and their response is different and depends upon the concentration of the oxidant and antioxidant, medium and reaction conditions (Santos-Sánchez et al., 2019). This could be the reason that some of the compounds from the library did not show any significant activity.

2.3.2. α-Amylase enzyme inhibition assay

All the synthesized compounds were evaluated concerning α amylase activity at various concentrations (200, 66.6, 22.2 and 7.40 µg/mL). Compounds activity with their IC_{50} values are presented in Table 3.

Among the tested compounds, **SH3** and **SH2** showed significant anti α amylase activity. These compounds exhibited more inhibitory activity than the standard, Acarbose. **SH3** and **SH2** were found to be effective at IC_{50} value of 9.48 ± 0.17 µg/mL and 10.17 ± 0.23 µg/mL, respectively than the standard (13.52 ± 0.19 µg/mL). These compounds inhibited α amylase activity 98.21 ± 0.41% and 89.11 ± 0.33% at 200 µg/mL concentration, respectively. Acarbose showed inhibitory effect by 87.89 ± 0.34% at the same concentration. **SH1** substituted with piperidine nucleus showed equipotent results to that of acarbose. **SH8**, **SH10**, **SH12** and **SH13** did not show any significant activity against the α-amylase enzyme. All the other compounds showed moderate anti α amylase activity.

Table 3 Dose dependent inhibitory effect of synthetic compounds at different Concentrations and their IC_{50} values.

Serial #	Compounds	α Amylase % enzyme inhibition at different Concentrations				IC_{50} [1] μg/mL
		200 μg/mL	66.6 μg/mL	22.22 μg/mL	7.40 μg/mL	
1	**SH1**	80.21 ± 0.31	63.00 ± 0.28	53.10 ± 0.33	44.00 ± 0.45	14.81 ± 0.21
2	**SH2**	89.14 ± 0.33	72 ± 0.21	52.00 ± 0.32	44.02 ± 0.34	10.17 ± 0.23
3	**SH3**	98.87 ± 0.41	83.00 ± 0.31	51.211 ± 0.18	40.01 ± 0.22	9.48 ± 0.17
4	**SH4**	65.99 ± 0.19	45.00 ± 0.38	38.11 ± 0.34	27.01 ± 0.21	99.08 ± 0.16
5	**SH5**	85.74 ± 0.21	61.12 ± 0.29	44.21 ± 0.28	33.01 ± 0.11	50.84 ± 0.15
6	**SH6**	50.48 ± 0.32	28.11 ± 0.16	19.00 ± 0.14	11.10 ± 0.21	193.03 ± 0.21
7	**SH7**	48.76 ± 0.22	31.31 ± 0.21	24.00 ± 0.17	13.00 ± 0.11	200.24 ± 0.28
8	**SH8**	24.79 ± 0.16	16.00 ± 0.23	11.11 ± 0.11	8.00 ± 0.16	499.48 ± 0.32
9	**SH9**	43.76 ± 0.22	32.13 ± 0.28	24.00 ± 0.21	15.00 ± 0.18	236.26 ± 0.32
10	**SH10**	20.07 ± 0.33	11.00 ± 0.18	6.69 ± 0.32	2.09 ± 0.09	537.61 ± 0.33
11	**SH11**	35.93 ± 0.28	24.00 ± 0.16	18.11 ± 0.28	12.01 ± 0.12	316.72 ± 0.29
12	**SH12**	18.81 ± 0.19	12.01 ± 0.13	9.35 ± 0.15	5.17 ± 0.32	678.40 ± 0.23
13	**SH13**	21.76 ± 0.26	14.00 ± 0.19	11.11 ± 0.21	8.14 ± 0.12	620.09 ± 0.27
14	**Blank**	0	0	0	0	–
15	**Acarbose**	87.89 ± 0.34	71.00 ± 0.31	53.10 ± 0.22	41.00 ± 0.21	13.52 ± 0.19

[1] IC_{50} is the concentration of the synthetic compounds that is required to inhibit 50% of the α amylase enzyme; values are described as Mean ± SEM (standard error of the mean, $n = 3$).

2.3.3. Anti microbial assay

2.3.3.1. Anti bacterial assay. The newly synthesized novel quinazolinone Mannich bases were investigated for their antibacterial activity. The antibacterial activity of the synthetic series was evaluated against five bacterial strains. Compounds that inhibited the bacterial growth to ≥ 50% were considered to be active and their MIC was determined by the disc diffusion method. Among the four strains, two gram-positive (*S. aureu, B. subtilis)* and three gram-negative strains (*E. coli, K. pneumoniae, and P. aeruginosa*) were used. None of the compounds showed any significant activity (% bacterial growth inhibition ≥ 50%) against gram-positive *Bacillus subtilis*. Some of them showed equipotent activity to standard, cefixime, and roxithromycin and some showed less value of MIC (more potent) than standard. The results of antibacterial activity and their MIC values are summarized in Table 4.

The results revealed that all of the newly synthesized Mannich bases were able to inhibit the bacterial growth *in vitro* and their MIC value range from 100 to 11.1 μg/mL. Among the synthesized compounds, **SH7** showed the best activity against all bacterial strains. **SH3** was the most potent against *P. aeruginosa*, having MIC value of 11.11 μg/mL and bacterial growth inhibition is up to 80%. Also, all other compounds showed moderate to good activity against bacterial strains. Differences

Table 4 Antibacterial evaluation of the synthetic compounds against gram-positive and gram-negative bacteria and their MIC values.

Compounds	% Inhibition against bacterial strain and minimum inhibitory concentration (MIC)[a]							
	Gram-positive		Gram-negative					
	S.aureus (ATCC-6538)	MIC (μg/mL)	*E.coli* (ATCC-25922)	MIC (μg/mL)	*K. pneumoniae* (ATCC-1705)	MIC (μg/mL)	*P.aeruginosa* (ATCC-25922)	MIC (μg/mL)
SH1	52 ± 1.2	100	38 ± 1.1	–	51 ± 1.0	100	74 ± 1.8	11.1
SH2	53 ± 1.0	100	35 ± 1.4	–	61 ± 1.5	33.3	78 ± 1.8	11.1
SH3	56 ± 1.0	100	31 ± 1.8	–	64 ± 1.2	33.3	80 ± 1.8	11.1
SH4	54 ± 1.5	100	29 ± 1.1	–	68 ± 1.5	33.3	69 ± 1.2	100
SH5	59 ± 1.5	100	18 ± 0.9	–	66 ± 1.5	33.3	72 ± 1.8	33.3
SH6	30 ± 1.1	–	19 ± 0.9	–	66 ± 1.3	33.3	55 ± 1.2	100
SH7	70 ± 1.8	11.1	74 ± 1.5	33.3	67 ± 1.5	100	70 ± 1.5	33.3
SH8	66 ± 1.5	33.3	42 ± 1.2	–	68 ± 1.8	100	77 ± 1.8	11.1
SH9	55 ± 1.1	100	36 ± 1.1	–	61 ± 1.8	100	69 ± 1.5	11.1
SH10	64 ± 1.8	33.3	39 ± 1.2	–	66 ± 1.6	33.3	76 ± 1.8	100
SH11	57 ± 1.1	100	25 ± 0.9	–	61 ± 1.5	33.3	79 ± 1.8	11.1
SH12	21 ± 1.0	–	14 ± 1.1	–	65 ± 1.8	33.3	76 ± 1.5	33.3
SH13	69 ± 2.2	11.1	43 ± 1.5	–	61 ± 1.1	100	67 ± 1.2	33.3
Blank	NA	–	NA	–	NA	–	NA	–
Cefixime	75 ± 1.7	4.25	70 ± 1.45	11.1	76 ± 1.6	11.1	70 ± 1.43	11.1
Roxithromycin	78 ± 1.6	11.1	70 ± 1.38	11.1	81 ± 1.8	11.1	67 ± 1.51	11.1

NA- not applicable. (–) indicates not applied.

[a] Values are Mean ± SD, n = 3. ≥ 50% of bacterial inhibition was considered for MIC.

in the composition of the cell wall of these gram-positive and gram-negative bacteria could be the basis for the lack of activity of the Mannich bases (Goszczyńska et al., 2015). The exact mechanism by which synthetic compounds inhibited bacterial growth is not known at the moment.

2.3.3.2. Anti fungal assay. All library compounds were tested against five fungal strains but only a few of them showed significant anti-fungal activity. Clotrimazole was chosen as a standard. The results are summarized in Table 5. The compounds having shown ≥12 mm zone of inhibition were selected for MIC (minimum inhibitory concentration).

SH4 and **SH5** showed significant activity against *A. flavus* strain at MIC values of 8 and 11 μg/mL, respectively. **SH5** and **SH6** showed good activity against *Mucor* strain at MIC values of 7 and 8, respectively. All the other compounds have not shown significant activity against fungal strains. None of the synthetic compounds showed activity (≥12 mm zone of inhibition) against *F. solani* strain.

2.3.4. Evaluation of cytotoxicity

2.3.4.1. Brine shrimp lethality assay. This is an economical and expeditious bioassay that may serve as a basic tool to scan bioactive compounds for further cancer cell line experiments on a large scale (Amanullah et al., 2012). The lethality of brine shrimp nauplii has a direct relationship with the cytotoxic nature of the tested compound (El-Gohary and Shaaban, 2014). All the Mannich bases were investigated for their cytotoxic evaluation by brine shrimp lethality assay. The results of the toxicity test of all the quinazolinone derivatives against brine shrimp nauplii and their LD_{50} values are summarized in Fig. 7.

The Mannich base **SH1, SH8** and **SH12** were found to be the most active with an LD_{50} value of 112.4, 119.2 and 129.3 μg/mL, respectively. **SH3, SH6, SH7** and **SH10** showed similar behavior against brine shrimp larvae at LD_{50} of 141.4 μg/mL. While the rest of the synthesized Mannich bases also exhibited good activity by killing the nauplii.

This approach is a useful tool to predict the cytotoxic potential of bioactive compounds and their response against brine shrimp larvae directly correlates to the mammalian system (Solis et al., 1993). DNA dependent RNA polymerase of *A. salina* has been reported to be similar to the mammalian type (Birndorf et al., 1975). The significant LD_{50} of the Mannich bases is an expression of the presence of cytotoxic functional groups which permits further research and investigation (Krishnaraju et al., 2005). From a pharmacological point of view, the compounds that have shown good cytotoxicity in brine shrimp bioassay are considered to be good antitumor agents (Carballo et al., 2002). This method has also applications in predicting the pesticidal and antimicrobial nature of the compounds (Sanchez et al., 1993).

2.3.4.2. Cytotoxicity against raw macrophages. MTT test was performed to determine the biocompatibility of the synthetic library. The MTT (3-(4, 5-dimethylthiazol-2-yl) 2, 5-diphenyl tetrazolium bromide) is a colorimetric method in which MTT is being converted into purple color formazan crystals by mitochondrial reductase enzyme present in the mitochondria of viable cells.

The % inhibition in cell viability of the quinazolinone derived Mannich bases were assessed *in vitro* by measuring the mitochondrial dehydrogenase activity on raw macrophages. The results of the biocompatibility assay were described in Table 6.

The synthetic compounds were tested at 100, 50, 10 and 1 μM concentration. Among the Mannich bases, **SH10** exhibited the most potent cytotoxic activity at IC_{50} 18.89 ± 0.10 of μM than the standard, doxorubicin i.e. 25.22 ± 0.13 μM. Followed by **SH7**, **SH12**, **SH1, SH3** and **SH9** at IC_{50} of 44.10 ± 0.18, 56.13 ± 0.09, 65.47 ± 0.02, 76.01 ± 0.47 and 76.06 ± 0.25 μM, respectively. All the other compounds did not show significant cytotoxic behavior. The compound **SH1**, substituted with piperidine is reported to have the antitumor potential (Das and da Silva, 2018). **SH9** having chlorine substitution indicates that it is a strong candidate for further

Table 5 Antifungal evaluation of the synthetic compounds and their MIC values.

Compounds	Zone of inhibition (mm) and minimum inhibitory concentration (MIC)[a]									
	A. fumigatus	MIC μg/mL	*F. solani*	MIC μg/mL	*Mucor*	MIC μg/mL	*A. flavus*	MIC μg/mL	*A. niger*	MIC μg/mL
SH1	NA	–	NA	–	NA	–	NA	–	NA	–
SH2	NA	–	NA	–	NA	–	NA	–	NA	–
SH3	NA	–	NA	–	5 ± 0.05	–	NA	–	NA	–
SH4	6 ± 0.5	–	NA	–	5 ± 0.5	–	15 ± 1.0	8	6 ± 1.0	–
SH5	NA	–	NA	–	12 ± 1.0	7	12 ± 0.9	11	NA	–
SH6	NA	–	NA	–	13 ± 1.2	8	NA	–	NA	–
SH7	9 ± 0.5	–	NA	–	NA	–	NA	–	NA	–
SH8	9 ± 0.5	–	NA	–	NA	–	NA	–	NA	–
SH9	NA	–	NA	–	NA	–	NA	–	NA	–
SH10	NA	–	NA	–	NA	–	NA	–	NA	–
SH11	NA	–	NA	–	NA	–	NA	–	NA	–
SH12	5 ± 0.5	–	NA	–	NA	–	9 ± 1.0	–	NA	–
SH13	5 ± 0.5	–	NA	–	8 ± 0.5	–	6 ± 0.5	–	NA	–
Blank	NA	–	NA	–	NA	–	NA	–	NA	–
Clotrimazole	19 ± 0.49	7 ± 0.31*	20 ± 0.43	6 ± 0.28*	16 ± 0.37	8 ± 0.26*	23 ± 0.29	8 ± 0.25*	28 ± 1.44	2.44 ± 0.91*

NA- not applicable. (*) indicate *p*-value < *0.05* compared to negative control; (–) indicates not applied.

[a] Values are Mean ± SD, n = 3. ≥ 12 mm zone of inhibition was considered for MIC.

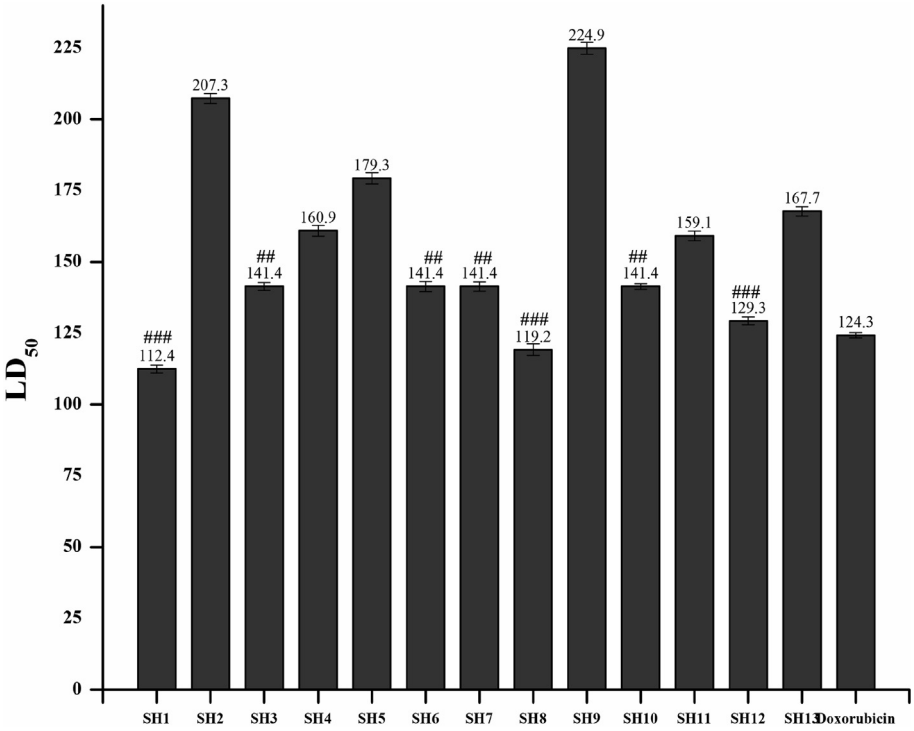

Fig. 7 Toxicity evaluation of the synthetic compounds by using Brine shrimp lethality assay. Values are expressed as Mean ± SEM (standard error of the mean, $n = 3$). ###/## indicates $p < 0.01$ and $p < 0.05$, respectively.

cytotoxic studies due to the presence of an electronegative atom (Abdo and Kamel, 2015). This is not a particular method to establish a direct correlation to anti-cancer activity but a positive correlation could be established based on cell cytotoxicity (Wiji Prasetyaningrum et al., 2018).

2.3.4.3. MTT assay against Hep-G2 cell lines. Among the thirteen newly synthesized quinazolinone derivatives, four were selected based on results from brine shrimp lethality and cell cytotoxicity assay. The compounds that have shown the least LD_{50} and IC_{50} values were considered to be the most deserving candidates for further analysis against Hep-G2 cancer cell lines. **SH1**, **SH7**, **SH10** and **SH12** showed potent cytotoxicity against brine shrimp nauplii at LD_{50} of 112.4, 141.4, 141.4 and 129.3 µg/mL, respectively. Moreover, the same compounds showed a significant % reduction in cell viability at IC_{50} of 65.47 ± 0.02, 44.10 ± 0.18, 18.89 ± 0.10 and 56.13 ± 0.09 µM, respectively. **SH8** possessed a significant lethality profile

Table 6 Cytotoxicity evaluation of synthetic library against raw macrophages at different concentrations.

Synthetic Library	% Inhibition in cell viability at different concentrations of synthetic compounds				IC_{50} (µM) [1]
	100 µM	50 µM	10 µM	1 µM	
SH1	65.81.20 ± 0.02	48.09.91 ± 0.16	25.46 ± 0.21	2.62 ± 0.27	65.47 ± 0.02###
SH2	49.31 ± 0.15	23.95 ± 0.22	14.99 ± 0.24	1.41 ± 0.27	103.47 ± 0.33
SH3	66.21 ± 0.11	30.99 ± 0.20	9.96 ± 0.25	4.43 ± 0.27	76.01 ± 0.47##
SH4	42.06 ± 0.17	21.94 ± 0.22	12.78 ± 0.24	1.01 ± 0.27	121.52 ± 0.35
SH5	29.78 ± 0.20	11.88 ± 0.25	7.15 ± 0.26	1.00 ± -0.28	178.04 ± 0.24
SH6	28.27 ± 0.21	15.6 ± 0.24	6.64 ± 0.26	0.51 ± 0.28	180.96 ± 0.27
SH7	71.72 ± 0.08	53.12 ± 0.08	41.76 ± 0.10	29.28 ± 0.10	44.10 ± 0.18###
SH8	44.37 ± 0.17	18.31 ± 0.23	10.97 ± 0.25	5.84 ± 0.26	121.54 ± 0.15
SH9	62.38 ± 0.19	36.22 ± 0.22	16.64 ± 0.24	12.73 ± 0.27	76.06 ± 0.25##
SH10	79.28 ± 0.21	62.25 ± 0.22	48.13 ± 0.25	42.98 ± 0.26	18.89 ± 0.10###
SH11	42.56 ± 0.17	28.27 ± 0.21	11.07 ± 0.25	4.23 ± 0.27	115.47 ± 0.11
SH12	75.87 ± 0.10	46.88 ± 0.15	30.93 ± 0.21	12.21 ± 0.27	56.13 ± 0.09###
SH13	34.11 ± 0.005	22.74 ± 0.01	12.68 ± 0.01	1.31 ± 0.01	148.57 ± 0.03
Control	100	100	100	100	0
Standard (Doxorubicin)	82.21 ± 0.27	64.00 ± 0.32	45.10 ± 0.26	36.12 ± 0.43	25.22 ± 0.13

[1] values are expressed as SEM (standard error of the mean, $n = 3$); ###/## indicate $p < 0.01$ and $p < 0.05$, respectively.

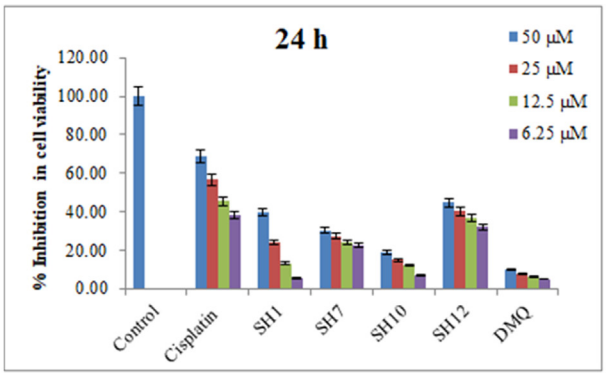

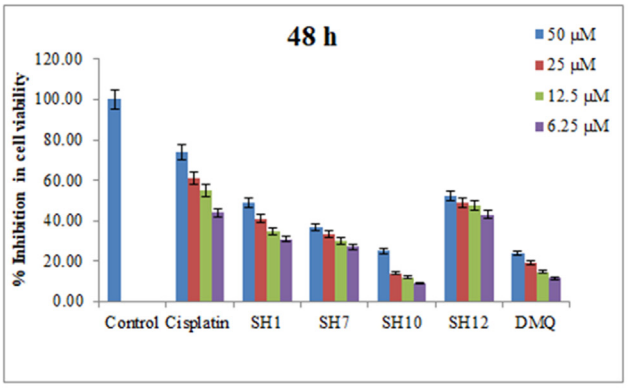

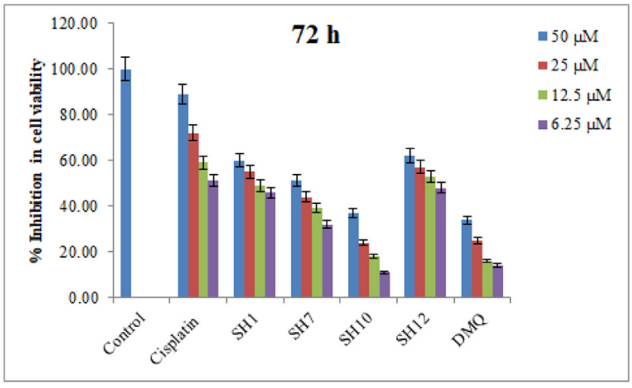

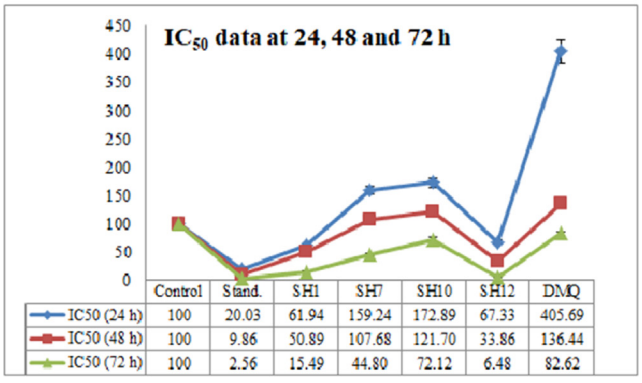

	Control	Stand.	SH1	SH7	SH10	SH12	DMQ
IC50 (24 h)	100	20.03	61.94	159.24	172.89	67.33	405.69
IC50 (48 h)	100	9.86	50.89	107.68	121.70	33.86	136.44
IC50 (72 h)	100	2.56	15.49	44.80	72.12	6.48	82.62

Fig. 8 A 3-(4, 5-dimethylthiazol-2-yl)-2, 5-diphenyltetrazolium bromide (MTT) spectrophotometric assay of the synthetic compounds at different µM concentrations in Hep G2 cells for 24, 48 and 72 h. IC_{50} data is also presented at 24, 48 and 72 h time intervals.

at LD_{50} of 119.2 µg/mL and it could be a suitable candidate for cancer cell lines but it has not any significant cell cytotoxicity and vice versa goes for **SH9** that showed good cytotoxicity against raw macrophages at IC_{50} of 76.06 ± 0.25 µM but has not shown lethality against brine shrimps.

The results were plotted against compounds concentrations and % inhibition in cell viability as described in Fig. 8. Cisplatin was taken as standard and Hep-G2 cells with DMEM media were taken as control. The anti-cancer effect of the synthetic compounds was also compared with the parent molecule (DMQ).

The compounds were tested for 24, 48 and 72 h intervals at 50, 25, 12.5 and 6.25 µM concentrations. The IC_{50} data was plotted. It was clear from the results that all the chosen compounds have shown moderate to good cytotoxic activity against Hep-G2 cells. The synthetic compounds have shown a dose-dependent response against cells. Most of the potent effects were observed at the 72 h period which might be due to the prolonged exposure of cancer cells to the synthetic compounds. IC_{50} data was calculated by using the GraphPad software. **SH12** showed the most potent effect at IC_{50} of 6.48 µM comparable to that of cisplatin (2.56 µM) at 72 h. **SH1** has also shown significant results at IC_{50} of 15.49 µM. **SH7** and **SH10** have also shown moderate results. From the literature survey, it is evident that compounds substituted with diphenylamine (**SH7**) and acetanilide (**SH10**) possess cytotoxic activity (Farooq et al., 2020). Quinazolinone heterocyclic compounds are reported to have the anti-proliferative potential (Poorirani et al., 2018; El-Sayed et al., 2017; Hassanzadeh et al., 2019), which on further derivatization with a cytotoxic compound will lead to an increase in cytotoxicity.

2.3.5. Evaluation of anti-inflammatory potential

2.3.5.1. Nitric oxide (NO) scavenging activity. A spectrophotometric assay was carried out to determine the nitrite level in the conditioned medium of LPS (lipopolysaccharides) treated macrophages. Griess reagent was used for this purpose. $NaNO_2$ was used as a standard and a standard curve was obtained to determine the nitrite concentration with the help of the regression equation (R^2 = 0.999). From Fig. 9, the % inhibition of the synthesized compounds towards NO generated by LPS induced macrophages was obtained. x designates the nitrite concentration in µM and y is the absorbance at 540 nm.

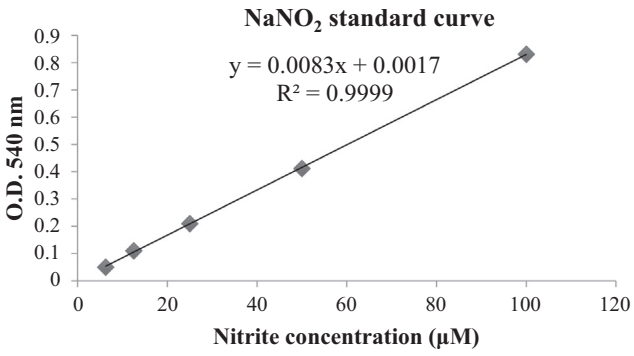

Fig. 9 $NaNO_2$ standard curve to obtain NO concentration.

The synthetic compounds were tested at 100, 50, 10 and 1 μM concentrations. All of the synthesized compounds showed the concentration-dependent response in terms of inhibition of NO production as summarized in Table 7.

From Table 7, it was evident that compound **SH12** showed the maximum NO inhibition at all concentrations followed by **SH1**, **SH10** and **SH13**. All these compounds' results are comparable to that of piroxicam. All the other compounds showed moderate to no activity against NO. It could be speculated that these synthetic compounds have the potential in the management of inflammatory conditions. Based on this hypothesis, these four Mannich bases were further tested on *in vivo* animal models to determine their *in vivo* anti-inflammatory potential.

2.3.5.2. In vivo anti-inflammatory activity. From the results of *in vitro* nitric oxide (NO) scavenging activity, four Mannich base derivatives of quinazolinone, having shown the maximum decrease in NO level, were chosen for *in vivo* study. A Dose-optimization study was conducted at first to optimize the dose. Animals were treated with 0.1 mg/kg, 1 mg/kg and 10 mg/kg dose of the tested compounds against 10 mg/kg dose of acetylsalicylic acid (ASA) as standard. From the dose optimization results, it was evident that 0.1 mg/kg and 1 mg/kg dose did not show any significant reduction in paw edema as compared to the 10 mg/kg dose of the respective compound (Fig. 10). So for this reason, 10 mg/kg dose is selected for further experiments.

The *in vivo* anti-inflammatory activity of **SH1**, **SH10**, **SH12** and **SH13** was performed by measuring the paw thickness. The synthetic compounds showed a significant decrease in paw thickness at different time intervals compared with the one treated with carrageenan (100 μL). **SH13** showed a decrease in paw edema and its results were comparable to that of standard. This is due to the presence of acetaminophen, an analog of Paracetamol, which belongs to a class of NSAID (non-steroidal anti-inflammatory agents) and is an analgesic and anti-inflammatory agent (Fresno et al., 2014). Acetaminophen inhibits cyclooxygenase (COX) enzyme, involved in the production and regulation of prostaglandins, mediators in inflammation (Simmons et al., 2000). All the other compounds

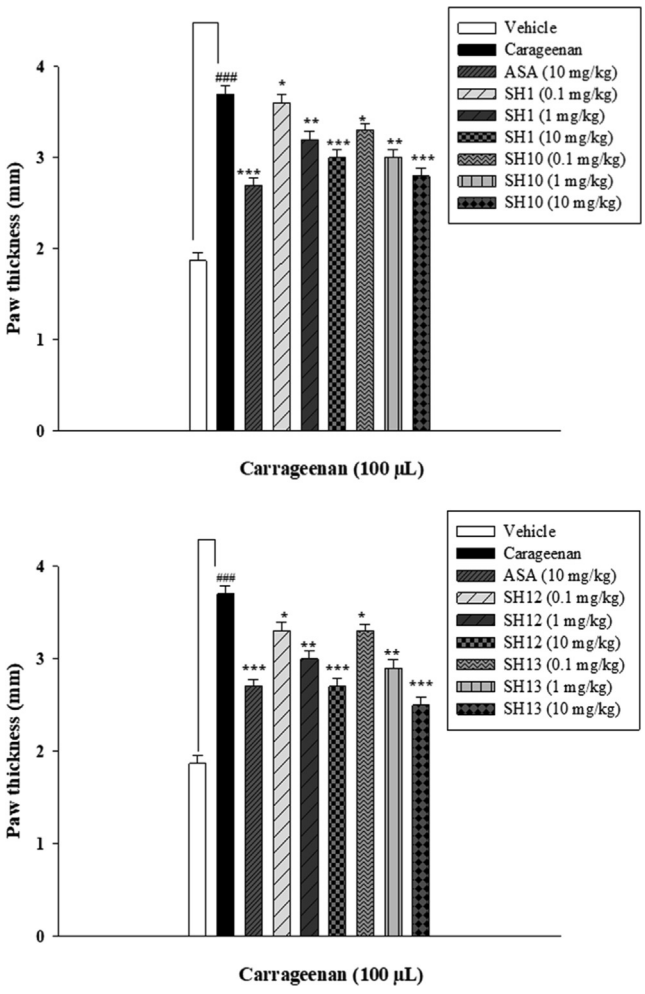

Fig. 10 Dose optimization of the synthesized compounds at 0.1, 1 and 10 mg/kg i.p. carrageenan-induced acute inflammatory model in mice (n = 5). The data are describes as Mean ± SEM (standard error of the mean), $^{*/**/***}$ indicates $p < 0.05$, $p < 0.01$ and $p < 0.001$, respectively. $^{###}$ indicates a significant difference from the carageenan treated group.

Table 7 NO (Nitric oxide) scavenging activity of the synthetic compounds at different concentrations.

Compounds	% NO (Nitric oxide) production at different concentrations (μM) (Mean ± SEM) [1]			
	100 μM	50 μM	10 μM	1 μM
SH1	30.06 ± 0.02	31.10 ± 0.02	31.88 ± 0.03	33.36 ± 0.01
SH2	28.22 ± 0.02	33.43 ± 0.01	38.40 ± 0.02	52.48 ± 0.04
SH3	21.84 ± 0.01	28.13 ± 0.01	34.43 ± 0.01	39.54 ± 0.02
SH4	35.23 ± 0.02	38.04 ± 0.02	44.87 ± 0.03	50.80 ± 0.02
SH5	24.65 ± 0.01	27.17 ± 0.02	29.10 ± 0.02	39.96 ± 0.01
SH6	29.41 ± 0.01	31.37 ± 0.01	34.74 ± 0.02	43.28 ± 0.02
SH7	46.26 ± 0.02	46.58 ± 0.02	62.09 ± 0.06	72.85 ± 0.08
SH8	28.31 ± 0.02	31.91 ± 0.03	32.21 ± 0.03	37.64 ± 0.03
SH9	31.85 ± 0.05	34.26 ± 0.04	45.53 ± 0.07	48.59 ± 0.06
SH10	27.34 ± 0.01	28.90 ± 0.02	33.24 ± 0.02	35.82 ± 0.02
SH11	26.72 ± 0.02	30.26 ± 0.02	34.72 ± 0.009	41.04 ± 0.01
SH12	23.20 ± 0.002	25.75 ± 0.008	31.37 ± 0.01	32.31 ± 0.01
SH13	14.63 ± 0.01	19.82 ± 0.01	27.74 ± 0.009	36.84 ± 0.01
Negative	100	100	100	100
Piroxicam	17.32 ± 0.01	19.43 ± 0.02	23.11 ± 0.02	28.39 ± 0.01

[1] Data are presented as SEM (standard error of the mean, $n = 3$).

Table 8 Acute *in vivo* anti-inflammatory evaluation of the synthetic compounds on carrageenaninduced inflammatory model ($n = 5$).

Compounds	Time after carrageenan injection [a]			
	0 h	2 h	4 h	6 h
Control	2.04 ± 0.07	2.05 ± 0.06	2.07 ± 0.04	2.10 ± 0.02
Carrageenan (100 µL)	2.11 ± 0.07	2.57 ± 0.08	2.75 ± 0.07	2.86 ± 0.05
Acetylsalicylic Acid (10 mg/kg)	2.14 ± 0.08	2.26 ± 0.05	2.32 ± 0.04	2.39 ± 0.02
SH1 (10 mg/kg)	2.21 ± 0.04	2.34 ± 0.04	2.70 ± 0.04	2.81 ± 0.06
SH10 (10 mg/kg)	2.22 ± 0.07	2.31 ± 0.08	2.38 ± 0.05	2.52 ± 0.05
SH12 (10 mg/kg)	2.19 ± 0.06	2.23 ± 0.06	2.31 ± 0.04	2.46 ± 0.07
SH13 (10 mg/kg)	2.11 ± 0.05	2.17 ± 0.01	2.27 ± 0.08	2.38 ± 0.07

[a] Readings were taken after every 2 h post carrageenan administration from 0 h to 6 h. All values are as Mean ± SD (standard deviation, $n = 5$).

showed moderate anti-inflammatory activity. The results are summarized in Table 8.

3. Materials and methodology

Unless otherwise noted, all commercially available solvents and chemicals were purchased from Sigma Aldrich and Merck, Germany. Analytical thin-layer chromatography (TLC) was performed with aluminum sheets silica gel 60 F254 (Merck), by using a solvent system, Ethyl acetate: pentane in 5: 2 ratio. The products were visualized with UV irradiation (254 nm). Gallenkamp melting point apparatus was used to determine the melting points with open capillaries, and are uncorrected. FTIR was recorded by the KBr pellets method by the PerkinElmer spectrum using the attenuated total reflectance (ATR). Nuclear magnetic resonance (NMR) spectra were recorded on an Agilent VNMR 400 (^{1}H NMR: 400 MHz, ^{13}C NMR: 101 MHz) or an Agilent VNMR 600 (^{1}H NMR: 600 MHz, ^{13}C NMR: 151 MHz) spectrometer. The chemical shifts are given in parts per million (ppm) relative to the residual solvent peak of the non-deuterated solvent ($CDCl_3$; ^{1}H NMR: $\delta = 7.26$ ppm; ^{13}C NMR: $\delta = 77.00$ ppm). The multiplicity was reported with the following abbreviations: s = singlet, d = doublet, t = triplet, m = multiplet, *p* = pentet, br = broad signal, dd = doublet of doublet, dt = doublet of triplet, ddt = doublet of doublet of triplet, td = triplet of doublet, tp = triplet of pentet, tdd = triplet of doublet of doublet. Mass spectra were recorded on a Finnigan SSQ 7000 spectrometer. The PE 2400 Series II CHNS/O Analyzer was used to determine the content of carbon, hydrogen, and nitrogen in organic materials.

3.1. General procedure for the synthesis of 3, 4-Dihydro-3-methyl-2(1H)-quinazolinone N-Mannich bases

Mannich bases of quinazolinone scaffold were synthesized by following the method of Farooq et al. (Farooq et al., 2020) with slight modifications. In a pressure glass tube, amines **1-13** (1.0 equiv, 0.5 mmol), formaldehyde **S** (2.0 equiv, 1 mmol) and 3, 4-Dihydro-3-methyl-2(1*H*)-quinazolinone nucleus **H** (1.0 equiv, 0.5 mmol) were taken and 3 mL of methanol was added into the pressure tube and the mixture was heated at 80 °C for ~ 5-7 h with constant stirring. 2 mol % HCl was added as a catalyst. The reaction progress and completion was monitored with TLC system (Ethyl acetate: Pentane in 5: 2 ratios). The reaction mixture was neutralized with $NaHCO_3$ solution and extracted with ethyl acetate (3 × 10 mL). The organic layer was dried over $MgSO_4$ and evaporated at reduced pressure. The product was purified by flash column chromatography (FCC) by using ethyl acetate: pentane in 5: 2 ratios.

The target compounds **SH1-SH13** were synthesized following the synthetic route mentioned in Scheme 2.

*3.1.1. 3-Methyl-1-(piperidin-1-ylmethyl)-3, 4-dihydroquinazolin-2(1H)-one (**SH1**)*

Yellow crystals; yield 82%; m.p. 230 °C, $R_f = 0.81$; IR (ATR) υ_{max} 3324, 3205, 3056, 2074, 1750, 1657, 1434, 1208, 941, 863, 716 cm^{-1}; ^{1}H NMR (600 MHz, $CDCl_3$) δ ppm 7.14–7.12 (m, 1H), 6.98 (s, 1H), 6.89 (td, $J = 7.5$, 1.2 Hz, 1H), 6.74 (dd, $J = 7.9$, 1.1 Hz, 1H), 4.43 (s, 2H), 4.10 (d, $J = 7.2$ Hz, 2H), 3.02 (s, 3H), 2.03 (s, 4H), 1.24 (t, $J = 7.2$ Hz, 6H); ^{13}C NMR (151 MHz, $CDCl_3$) δ ppm 154.79, 137.73, 128.10, 127.81, 125.26, 121.63, 113.80, 60.37, 50.84, 50.38, 35.60, 34.47, 25.58, 24.04; EIMS *m/z* 259.21 (M+); Anal. ($C_{15}H_{21}N_3O$): C 69.47, H 8.16, N 16.20, Found: C 69.39, H 8.15, N 16.21.

*3.1.2. 3-Methyl-1-(morpholino methyl)-3,4-dihydroquinazolin-2(1H)-one (**SH2**)*

Yellow crystals; yield 88%; m.p. 241 249 °C, $R_f = 0.79$; IR (ATR) υ_{max} 3144, 2493, 2113, 1923, 1748, 1631, 1493, 1301, 1172, 1101, 870, 696 cm^{-1}; ^{1}H NMR (600 MHz, $CDCl_3$) δ ppm 7.13 (m, 1H), 6.99 (m, 1H), 6.89 (td, $J = 7.4$, 1.1 Hz, 1H), 6.75 (dd, $J = 7.9$, 1.1 Hz, 1H), 4.43 (s, 2H), 4.10 (q, $J = 7.1$ Hz, 2H),3.03–3.02 (m, 4H), 2.03 (s, 3H), 1.24 (t, 4H); ^{13}C NMR (151 MHz, $CDCl_3$) δ ppm 154.84, 137.99, 128.13, 125.26, 122.41, 121.63, 113.83, 60.38, 50.84, 50.38, 34.47; EIMS *m/z* 261 (M+); Anal. ($C_{14}H_{19}N_3O_2$): C 64.35, H 7.33, N 16.08, Found: C 64.39, H 7.32, N 16.06.

*3.1.3. 3-Methyl-1-(pyrrolidin-1-ylmethyl)-3,4-dihydroquinazolin-2(1H)-one (**SH3**)*

White crystals; yield 79%; m.p. 218 223 °C; $R_f = 0.83$; IR (ATR) υ_{max} 3055, 2325, 1923, 1748, 1631, 1493, 1393, 1207, 1028, 865, 758 cm^{-1}; ^{1}H NMR (600 MHz, $CDCl_3$) δ ppm 7.14 (td, $J = 7.7$, 1.4 Hz, 1H), 7.00 (d, $J = 7.3$ Hz, 1H), 6.90 (td, $J = 7.5$, 1.1 Hz, 1H), 6.73 (dd, $J = 7.9$, 1.1 Hz, 1H), 4.43 (s, 2H), 4.11 (d, $J = 7.1$ Hz, 2H), 3.02 (s, 3H), 2.03 (s, 4H), 1.24 (t, $J = 7.2$ Hz, 4H); ^{13}C NMR (151 MHz,

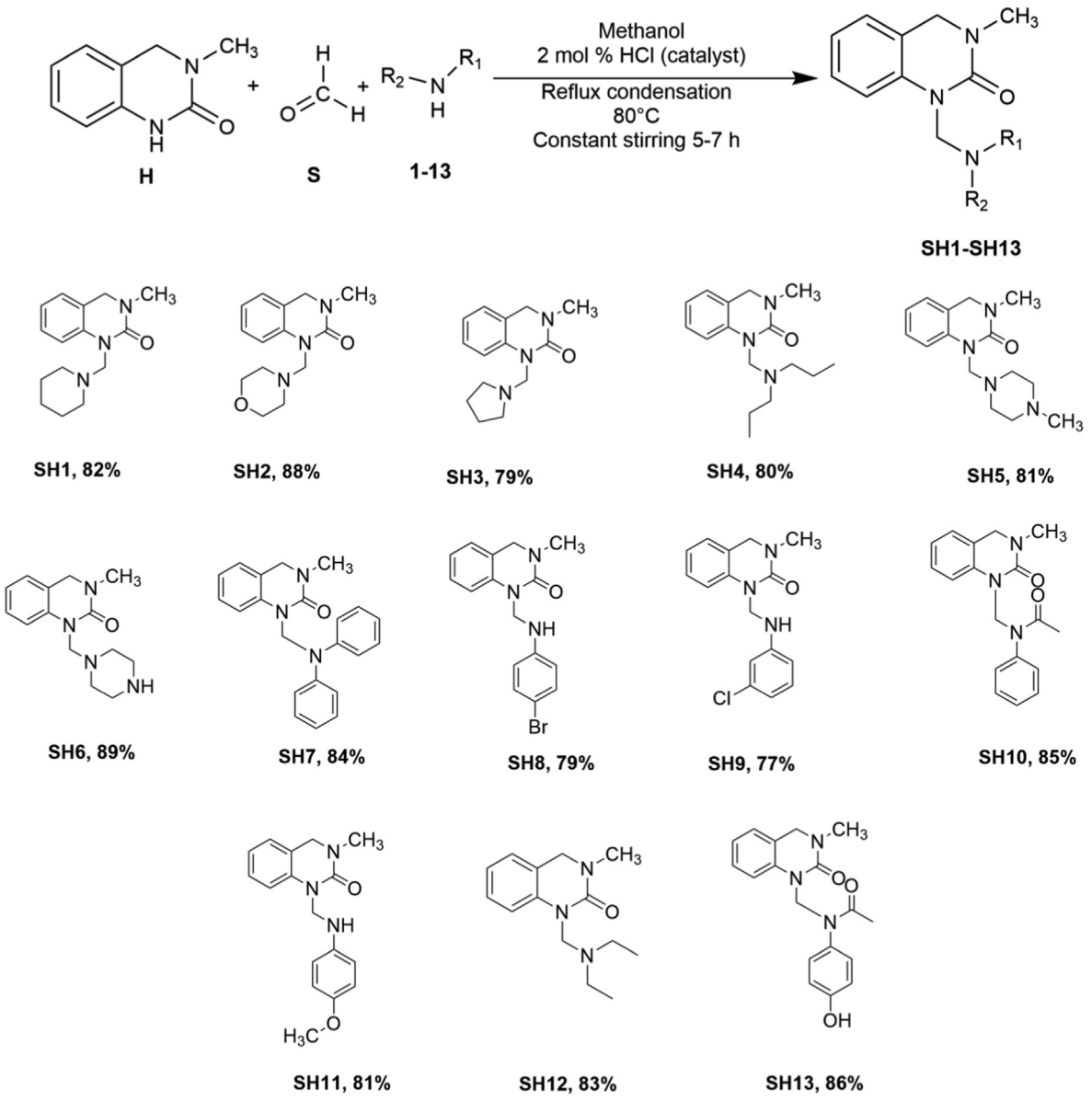

Scheme 2 Synthesis of compounds **SH1 SH13.** Reaction conditions: **H** (1.0 equiv), **S** (2.0 equiv), **1 13 (**2.0 equiv); 3 mL Methanol, 2 mol % HCl, 80 °C (oil bath). Yields obtained after product purification.

$CDCl_3$) δ ppm 154.70, 137.13, 128.15, 125.29, 121.67, 117.30, 113.75, 60.38, 50.84, 34.49, 14.18; EIMS *m*/*z* 245.31 (M +); Anal. ($C_{14}H_{19}N_3O$): C 68.54, H 7.81, N 17.13, Found: C 68.54, H 17.79, N 17.13.

*3.1.4. 1-((Dipropyl amino) methyl)-3-methyl-3, 4-dihydroquinazolin-2(1H)-one (**SH4**)*

Half white crystals; yield 80%; m.p. 228 °C; R_f = 0.89; IR (ATR) υ_{max} 3204, 3057, 2918, 2323, 2072, 1871, 1658, 1433, 1250, 1035, 921, 781, 716 cm^{-1}; ^1H NMR (400 MHz, $CDCl_3$) δ ppm 7.39–7.35 (m, 1H), 7.24–7.17 (m, 2H), 7.10 (td, *J* = 7.4, 2.2 Hz, 1H), 4.44 (d, *J* = 0.9 Hz, 2H), 4.00 (s, 2H), 3.08 (s, 3H), 2.50 (t, *J* = 7.5 Hz, 4H), 1.57 (ddt, *J* = 14.2, 7.5, 6.7 Hz, 4H), 0.92 (t, *J* = 6.7 Hz, 6H); ^{13}C NMR (101 MHz, $CDCl_3$) δ ppm 154.78, 138.77, 128.10, 127.69, 121.66, 119.60, 119.26, 62.95, 58.06, 50.13, 35.21, 21.31, 11.85; EIMS *m*/*z* 275.34 (M +); Anal. ($C_{16}H_{25}N_3O$): C 69.78, H 9.15, N 15.26, Found: C 69.80, H 9.15, N 15.24.

*3.1.5. 3-Methyl-1-((4-methylpiperazin-1-yl) methyl)-3, 4-dihydroquinazolin-2(1H)-one (**SH5**)*

White crystals; yield 81%; m.p. 268 °C; R_f = 0.89; IR (ATR) υ_{max} 3204, 3058, 2324, 1655, 1523, 1433, 1251, 1035, 864, 781, 715 cm^{-1}; ^1H NMR (600 MHz, $CDCl_3$) δ ppm 7.15 (td, *J* = 7.7, 1.3 Hz, 1H), 7.02–7.00 (m, 1H), 6.91 (td, *J* = 7.5, 1.1 Hz, 1H), 6.70 (dd, *J* = 7.9, 1.1 Hz, 1H), 4.44 (s, 2H), 4.11 (d, *J* = 7.1 Hz, 2H), 3.03 (s, 3H), 2.04 (s, 4H), 1.25 (t, *J* = 7.2 Hz, 7H); ^{13}C NMR (151 MHz, $CDCl_3$) δ ppm 154.49, 137.02, 128.18, 125.35, 121.77, 117.35, 113.63,60.36, 50.84, 34.51; EIMS *m*/*z* 274.31 (M+); Anal. ($C_{15}H_{22}N_4O$): C 65.67, H 8.08, N 20.42, Found: C 65.69, H 8.10, N 20.41.

*3.1.6. 3-Methyl-1-(piperazin-1-ylmethyl)-3, 4-dihydroquinazolin-2(1H)-one (**SH6**)*

White powder; yield 89%; m.p. 273 277 °C; R_f = 0.87; IR (ATR) υ_{max} 3204, 2935, 2794, 1923, 1661, 1606, 1447, 1347, 1282, 1164, 1010, 917, 830 cm^{-1}; ^1H NMR (400 MHz, $CDCl_3$) δ ppm 7.14–7.10 (m, 1H), 6.99 (d, J = 7.5 Hz, 1H), 6.89 (td, J = 7.5, 1.1 Hz, 1H), 6.68 (dd, J = 7.9, 1.1 Hz, 1H), 4.42 (s, 2H), 4.03 (s, 3H), 3.68 (q, J = 7.0 Hz, 4H), 3.00 (s, 4H), 2.65 (s, 2H), 1.16 (s, 1H); ^{13}C NMR (101 MHz, $CDCl_3$) δ ppm 154.48, 136.99, 128.15, 125.32, 121.75, 117.32, 113.62, 64.34, 51.43, 50.24, 49.46, 34.49; EIMS m/z 260.37 (M+); Anal. ($C_{14}H_{20}N_4O$): C 64.59, H 7.74, N 21.52, Found: C 64.54, H 7.72, N 21.52.

*3.1.7. 1-((Diphenylamino) methyl)-3-methyl-3, 4-dihydroquinazolin-2(1H)-one (**SH7**)*

Green powder; yield 84%; m.p. 335–342 °C; R_f = 0.93; IR (ATR) υ_{max} 3205, 3058, 2319, 1915, 1794, 1661, 1605, 1495, 1402, 1306, 1251, 1036, 921, 864, 750 cm^{-1}; ^1H NMR (600 MHz, $CDCl_3$) δ ppm 8.08 (s, 1H), 7.29–7.24 (m, 4H), 7.13–7.10 (m, 4H), 7.07–6.91 (m, 3H), 6.91 (tt, J = 7.5, 1.7 Hz, 1H), 6.73 (dd, J = 7.9, 1.1 Hz, 1H), 4.44 (s, 2H), 4.14–4.10 (m, 2H), 3.03 (s, 3H); ^{13}C NMR (151 MHz, $CDCl_3$) δ ppm 154.68, 137.74, 129.24, 129.22, 129.15, 122.30, 121.45, 121.37, 120.88, 117.73, 50.85, 34.50; EIMS m/z 343.30 (M+); Anal. ($C_{22}H_{21}N_3O$): C 76.94, H 6.16, N 12.24, Found: C 76.93, H 6.18, N 12.24.

*3.1.8. 1-(((4-Bromophenyl) amino) methyl)-3-methyl-3, 4-dihydroquinazolin-2(1H)-one (**SH8**)*

White powder; yield 79; m.p. 340 345 °C; R_f = 0.91; IR (ATR) υ_{max} 3322, 3205, 3058, 2862, 2085, 1870, 1659, 1604, 1489, 1402, 1306, 1240, 1075, 1034, 998, 881, 750 cm^{-1}; ^1H NMR (600 MHz, $CDCl_3$) δ ppm 7.86 (s, 1H), 7.32–7.25 (m, 1H), 7.14 (td, J = 7.7, 1.3 Hz, 1H), 7.01–7.00 (m, 1H), 6.94–6.90 (m, 2H), 6.71 (dd, J = 7.9, 1.0 Hz, 2H), 4.80 (s, 2H), 3.70 (q, J = 7.0 Hz, 2H), 3.47 (s, 1H), 3.03 (s, 3H); ^{13}C NMR (151 MHz, $CDCl_3$) δ ppm 154.61, 145.83, 137.03, 131.71, 128.18, 127.45, 122.03, 121.76, 119.28, 116.33, 111.99, 62.36, 50.85, 34.51; EIMS m/z 344.23 (M+); Anal. ($C_{16}H_{16}BrN_3O$): C 55.51, H 4.66, N 12.14, Found: C 55.50, H 4.65, N 12.14.

*3.1.9. 1-(((3-Chlorophenyl) amino) methyl)-3-methyl-3, 4-dihydroquinazolin-2(1H)-one (**SH9**)*

Maroon powder; yield 77%; m.p. 318 °C; R_f = 0.79; IR (ATR) υ_{max} 3321, 3204, 3058, 2319, 2087, 1661, 1606, 1523, 1493, 1402, 1305, 1251, 1209, 1152, 1036, 923, 864, 751 cm^{-1}; ^1H NMR (400 MHz, $CDCl_3$) δ ppm 7.13 (dt, J = 8.1, 1.4 Hz, 1H), 7.03–6.87 (m, 3H), 6.85–6.81 (m, 1H), 6.69–6.62 (m, 2H), 6.56–6.51 (m, 1H), 4.83 (s, 2H), 4.43 (s, 2H), 3.01 (s, 3H), 2.15 (s, 1H); ^{13}C NMR (101 MHz, $CDCl_3$) δ ppm 132.07, 128.56, 128.46, 128.21, 125.42, 125.22, 123.09, 122.73, 121.92, 114.77, 113.81, 113.46, 50.81, 50.22, 35.61; EIMS m/z 310.10 (M+); Anal. ($C_{16}H_{16}ClN_3O$): C 63.68, H 5.34, N 13.92, Found: C 63.67, H 5.31, N 13.89.

*3.1.10. N-((3-methyl-2-oxo-3, 4-dihydroquinazolin-1(2H)-yl) methyl)-N-phenylacetamide (**SH10**)*

White crystals; yield 85%; m.p. 326 °C; R_f = 0.86; IR (ATR) υ_{max} 3203, 3152, 3059, 2922, 2865, 2087, 1874, 1658, 1604, 1524, 1490, 1433, 1306, 1252, 1208, 1153, 1035, 863 cm^{-1};^1H NMR (600 MHz, $CDCl_3$) δ ppm 7.76 (s, 1H), 7.51–7.50 (m, 2H), 7.30–7.26 (m, 2H), 7.14 (ddd, J = 8.5, 7.4, 1.3 Hz, 1H), 7.00 (dd, J = 7.4, 1.3 Hz, 1H), 6.91 (td, J = 7.5, 1.1 Hz, 1H), 6.71 (dd, J = 7.9, 1.1 Hz, 1H), 4.43 (s, 2H), 4.11 (q, J = 7.1 Hz, 2H), 3.02 (s, 3H), 1.25 (t, J = 7.1 Hz, 3H); ^{13}C NMR (151 MHz, $CDCl_3$) δ ppm 171.08, 154.52, 137.08, 128.41, 128.14, 125.31, 122.35, 121.70, 117.34, 113.91, 113.65, 60.34, 50.83, 20.99, 14.15; EIMS m/z 310.14 (M+); Anal. ($C_{18}H_{19}N_3O_2$): C 69.88, H 6.19, N 13.58, Found: C 69.87, H 6.21, N 13.59.

*3.1.11. 1-(((4-Methoxyphenyl) amino) methyl)-3-methyl-3, 4-dihydroquinazolin-2(1H)-one (**SH11**)*

Yellow powder; yield 81%; m.p. 315 318 °C; R_f = 0.76; IR (ATR) υ_{max} 3321, 3205, 3058, 2912, 2590, 2326, 2113, 1909, 1747, 1660, 1502, 1403, 1259, 1170, 1023, 922, 828 cm^{-1}; ^1H NMR (400 MHz, $CDCl_3$) δ ppm 7.21–7.11 (m, 2H), 7.04 (t, J = 8.3 Hz, 3H), 6.95 (td, J = 7.4, 1.1 Hz, 1H), 6.82–6.79 (m, 1H), 6.70 (dd, J = 7.9, 1.1 Hz, 1H), 4.70 (s, 2H), 4.47 (s, 2H), 3.77 (s, 3H), 3.06 (s, 3H), 2.07 (s, 1H); ^{13}C NMR (101 MHz, $CDCl_3$) δ ppm 142.64, 136.99, 128.22, 125.44, 121.85, 120.08, 117.45, 114.45, 113.53, 55.55, 50.87, 34.56; EIMS m/z 297.31 (M +); Anal. ($C_{17}H_{19}N_3O_2$): C 68.67, H 6.44, N 14.13, Found: C 68.69, H 6.54, N 14.12.

*3.1.12. 1-((Diethylamino) methyl)-3-methyl-3, 4-dihydroquinazolin-2(1H)-one (**SH12**)*

Yellow crystals; yield 83%; m.p. 198 203 °C; R_f = 0.83; IR (ATR) υ_{max} 3321, 3206, 3060, 2915, 2774, 2482, 2080, 1962, 1751, 1658, 1605, 1522, 1401, 1328, 1251, 1154, 1035, 921, 863 cm^{-1}; ^1H NMR (600 MHz, $CDCl_3$) δ ppm 7.12 (qd, J = 8.1, 1.2 Hz, 1H), 6.98 (dd, J = 7.5, 1.2 Hz, 1H), 6.88 (td, J = 7.5, 1.1 Hz, 1H), 6.71 (dd, J = 8.0, 1.1 Hz, 1H), 4.41 (s, 2H), 3.00 (s, 2H), 2.54 (q, J = 7.2 Hz, 5H), 1.09–1.06 (m, 5H), 0.96 (s, 3H); ^{13}C NMR (151 MHz, $CDCl_3$) δ ppm 154.68, 138.79, 128.12, 127.88, 121.80, 121.67, 117.28, 61.38, 50.41, 45.03, 34.46, 11.73; EIMS m/z 247.34 (M+); Anal. ($C_{14}H_{21}N_3O$): C 67.98, H 8.56, N 16.99, Found: C 67.99, H 8.54, N 16.97.

*3.1.13. N-(4-hydroxyphenyl)-N-((3-methyl-2-oxo-3, 4-dihydroquinazolin-1(2H)-yl)methyl)acetamide (**SH13**)*

Half white crystals; yield 86%; m.p. 428 °C; R_f = 0.93; IR (ATR) υ_{max} 3202, 3123, 3057, 2916, 2589, 2324, 2112, 1872, 1799, 1748, 1656, 1606, 1495, 1439, 1402, 1330, 1276, 1215, 1107, 1036, 921, 827 cm^{-1}; ^1H NMR (600 MHz, $CDCl_3$) δ ppm 9.95 (s, 1H), 7.40–7.37 (m, 1H), 7.21–7.15 (m, 3H), 7.11–7.07 (m, 2H), 6.89–6.87 (m, 2H), 5.02 (s, 2H), 4.44 (d, J = 0.9 Hz, 2H), 3.13 (s, 3H), 1.90 (s, 3H); ^{13}C NMR (151 MHz, $CDCl_3$) δ ppm 171.17, 154.42, 136.91, 128.19, 125.38, 122.19, 121.84, 117.35, 116.62, 116.09, 115.63, 113.60, 60.39, 50.84, 34.53, 24.24, 21.02, 14.17; EIMS m/z 325.33 (M+); Anal. ($C_{18}H_{19}N_3O_3$): C 66.45, H 5.89, N 12.91, Found: C 66.44, H 5.89, N 12.90.

3.2. In silico studies

A computational software was used to assess the pharmacokinetics (absorption, distribution, metabolism, excretion) behav-

ior of the newly synthesized compounds **(SH1-SH13).** By using the *in silico* method, we assessed the following five parameters of the synthesized compounds: molecular weight (MW), molar refractivity logarithm of the partition coefficient (iLOGP), Alog P, hydrogen bond donors (HBD) and hydrogen bond acceptors (HBA) to determine the drug-likeness of the synthesized compounds and their probability to follow Lipinski's rule of five (RO5) (Software, 2020).

3.3. Bioevaluation

3.3.1. Antioxidant assay

3.3.1.1. DPPH assay. The % FRSA (free radical scavenging activity) of the synthetic compounds **(SH1-SH13)** was determined by using the method of Tai *et al*. (Tai et al., 2011) with slight modifications. The method is based to determine the potential of the synthetic compounds to quench free radical i.e. DPPH. Assay was performed in a 96-well plate, by adding the compounds in three-fold concentration of 200, 66.6, 22.2 and 7.4 µg/mL. After adding the compounds in a 96-well plate, DPPH solution was added to make up the final volume up to 200 µL. Ascorbic acid and DMSO were taken as positive and negative controls, respectively. The absorbance was taken at 515 nm using a microplate reader (ELx800 BioTek). The percentage of scavenging activity was calculated by the given formula:

$$\%\ \text{scavenging activity} = (1 - \text{Ab}_s/\text{Ab}_c) \times 100$$

Ab_s = sample's absorbance; Ab_c = control's absorbance.

3.3.1.2. Determination of total antioxidant capacity (TAC). TAC assay was performed by using the phosphomolybdenum based method (Aguilar Urbano et al., 2013). The reduction of molybdenum VI to molybdenum V results in the formation of a green-colored phosphate-molybdenum complex that gives absorption at 630 nm. In a 96-well plate; 180 µL TAC reagents and 20 µL of the sample solution was added to make up a final volume of 200 µL. 96-well plate is incubated at 95 °C for 90 min in the water bath and cooled at room temperature. Results were calculated as µg AAE/mg.

3.3.1.3. Determination of total reducing power (TRP). The assay is based on the reduction of Fe^{+3} to Fe^{+2}. The method described by Khan *et al*. was used with slight modifications. The stock solution of the compounds was prepared in DMSO (4 mg/mL DMSO). 100 µL test sample was taken in an Eppendrof tube and 200 µL of phosphate buffer (0.2 mol/L, pH 6.6) and 250 µL of 1% potassium ferricyanide $[K_3Fe\ CN)_6]$ was added. This was allowed to incubate at 50 °C for 20 mins. After incubation, 200 µL of 10% trichloroacetic acid (TCA) was added to the mixture. The mixture was centrifuged at 3000 rpm at room temperature for 10 min. After centrifugation, 150 µL supernatant was transferred to a microplate having $FeCl_3$ (50 µL, 0.1%) and absorbance was taken at 700 nm (Khan et al., 2015). Results were calculated as µg AAE/mg.

3.3.2. α-Amylase enzyme inhibition assay

An *in vitro* α-amylase enzyme inhibitory assay was performed by the standard protocol (Kim et al., 2000). In each well of a 96-well plate, test samples (4 mg/mL DMSO) were added to a final concentration of 200 µg/mL.

To this, 25 mL α-amylase enzyme solution, 40 µL starch, and 15 µL phosphate buffer were added stepwise. The plate was incubated at 50 °C for 30 min. after incubation, 20 µL HCl (1 M) and 90 µL iodine solution were added and reading was taken at 540 nm. Acarbose and DMSO were taken as positive and negative controls, respectively. The formula used to calculate the percent enzyme inhibition is:

$$\%\ \text{Enzyme inhibition} = \left[(\text{As} - \text{An})\tilde{A} \cdot (\text{Ab} - \text{An})\right] \times 100$$

As = sample's absorbance; An = negative's absorbance; Ab = blank's absorbance.

Synthetic compounds with a % enzyme inhibition $\geq$ 50% were taken at three-fold concentrations of 200, 66.6, 22.2, and 7.41 µg/mL and their IC_{50} was calculated.

3.3.3. Anti-microbial assay

3.3.3.1. Anti-bacterial assay. All the synthesized compounds were evaluated to determine their antibacterial potential against gram-positive and gram-negative bacteria by the method described by Gao *et al*. (Gao et al., 2012) with slight modifications. Five bacterial strains used were: *Staphylococcus aureus* (ATCC-6538), *Bacillus subtilis* (ATCC-6633), *Klebsiella pneumniae* (ATCC-1705), *E.coli* (ATCC-25922) and *Pseudomonas aeruginosa* (ATCC-15442). 20 mg/mL stock solution of the synthetic compounds was prepared in DMSO and made up to a final concentration of 100, 33.3, 11.1, and 3.7 µg/mL. Initial screening was performed by microtitre plate-based antibacterial assay. Bacterial strains were inoculated with 10 mL of TSB and incubated for 24 h at 37 °C. The bacterial inoculum was prepared with pre-adjusted density (1×10^8 CFU/mL). Reading was taken at 0 h and 24 h incubation. Cefixime monohydrate and roxithromycin were taken as a positive control, while DMSO as a blank or negative control. The assay was run in triplicate. Plates were observed under a microplate reader at 630 nm wavelength. The corresponding 50% inhibitory concentration of each synthetic compound was calculated using the following formula:

$$\%\ \text{inhibition} = (1 - T_s/T_c) \times 100$$

where T_s is the turbidity of the sample well and T_c is the turbidity of control well.

3.3.3.2. Anti-fungal assay. The synthetic compounds were evaluated against five fungal strains: *Aspergillus flavus* (FCBP-0064), *Aspergillus fumigatus* (FCBP-1264), *Aspergillus niger* (FCBP-0198), *Fusarium solani* (FCBP-0291), *Mucor species* (FCBP-0300). Stock solutions of compounds (20 mg/mL) were prepared in DMSO. The Agar disc diffusion method was chosen for preliminary screening of antifungal activity of synthetic compounds. Clotrimazole was served as positive while DMSO as a negative control. Separate petri plates having sterile SDA (20–25 mL) were swabbed with an aliquot of 100 µL spore suspension from each fungal strain harvested in 0.02% (v/v) Tween 20 solution. On sterile filter paper discs, test samples were applied and the discs were placed on the seeded agar plates. Plates were incubated at 37 °C for 24–48 h with periodic observation of inhibition zones (Katircioglu et al., 2006).

3.3.4. Evaluation of cell cytotoxicity

3.3.4.1. Brine shrimp lethality assay. Brine shrimp lethality assay was performed to determine the cytotoxicity of the syn-

thetic compounds. Brine shrimp eggs were hatched and in a 96-well plate, 150 µL of artificial seawater was added. To this, 10 nauplii were added. Synthetic compounds at concentrations of 400, 200, 100, and 50 µg/mL were added into each well and the final volume of the well plate was made up to 200 µL by artificial seawater. The well plate was left uncovered under a lamp for 24 h. After 24 h, the number of surviving nauplii was counted under a microscope. The test was repeated in triplicate (McLaughlin, 1982). Using GraphPad Prism, the lethality concentration (LD_{50}) was assessed at 95% confidence intervals. The percentage mortality (%M) was also calculated by dividing the number of dead nauplii by the total number multiplied by 100.

3.3.4.2. Cytotoxicity against raw macrophages. The cytotoxic potential of the synthetic library was assessed by using an MTT 3-(4,5-dimethyl thiazole-2-yl)-2,5- diphenyl tetrazolium bromide assay (Khan et al., 2011). In a 96-well plate, extracted macrophages (peritoneal cavity of albino rats) were plated at a density of 1×10^6 per well and incubated in a 5% CO_2 incubator at 37 °C for 24 h. The stock solution of the compounds was prepared at a concentration of 100 µM and further dilutions were made from it at concentrations of 50, 10, and 1 µM. After incubation, 20 µL of MTT (1 mg/mL in PBS) was added to each well and incubated under the same conditions for another 2 h. Mitochondrial succinate dehydrogenase converted MTT in viable cells into purple formazan crystals. The formazan crystals were then solubilized in 100 µL solubilizing agent (DMSO), and the absorbance was measured at 570 nm. The % cell viability was calculated by the following formula;

$$\%\ \text{cell viability} = (\text{abs}_{\text{samble}} - \text{abs}_{\text{blank}})/(\text{abs}_{\text{control}} - \text{abs}_{\text{blank}}) \times 100$$

3.3.4.3. MTT assay against Hep-G2 cell lines. Hep-G2 cell line experiments were performed in the Immunology Lab of the National Institute of Health (NIH), Islamabad, Pakistan. Human hepatocellular carcinoma cells Hep-G2 (ATCC HB-8065) were cultured in Dulbecco's modified Eagle's medium (DMEM), comprising 10% fetal calf serum (10% FCS) and supplemented with 2 mM L-glutamine, 100 U/mL penicillin, 100 µg/mL streptomycin and 1 mM Na pyruvate, at 37 °C in a humidified 5% CO_2 incubator.

The tetrazolium dye 3-(4, 5-dimethyl thiazolyl-2)-2, 5-diphenyltetrazolium bromide (MTT) was used to assess the cytotoxic potential of the test compounds by using the method of Horiuchi et al. (Horiuchi et al., 1988) with slight modifications. Hep-G2 cells, in a density of 1×10^6 (>90% cell viability), were cultured in a 96-well plate and treated with different concentrations of the test compounds for 24, 48, and 72 h. 10 µL of MTT (1 mg/mL) were added per well followed by incubation for 4 h. Insoluble formazan crystals were dissolved by adding 100 µL of the solubilizing agent (DMSO). Cells were then incubated for another 2 h. Absorbance was measured at 570 nm by a microplate reader (Senthilraja and Kathiresan, 2015). Untreated Hep-G2 cells were taken as controls and DMSO as a negative.

$$\%\ \text{cell viability} = (\text{abs}_{\text{samble}} - \text{abs}_{\text{blank}})/(\text{abs}_{\text{control}} - \text{abs}_{\text{blank}}) \times 100$$

3.3.5. Evaluation of anti-inflammatory potential

3.3.5.1. Nitric oxide (NO) scavenging assay. The *in vitro* anti-inflammatory effect of the synthesized compounds in murine macrophages was evaluated by using the Griess reaction method, described previously (Ahn et al., 2005). Shortly, macrophages were plated in a 96-well plate at a density of 1×10^6 and incubated in a 5% CO_2 incubator at 37 °C for 24 h, pretreated with different concentrations (100 µM, 50 µM, 10 µM and 1 µM) of synthetic compounds for another 2 h and treated with LPS (1 µg/mL) for an additional 18 h. Equal volumes of Griess reagent (1% sulphanilamide in 50% phosphoric acid and 0.1% naphthyl ethylenediamine dihydrochloride in distilled water and vortexed) and culture medium were mixed and the absorbance was taken at 540 nm. Lipopolysaccharide (LPS) was taken as a blank and piroxicam was taken as a positive control. The regression equation is used to determine the NO concentration.

3.3.5.2. In vivo anti-inflammatory activity. At 7–8 weeks old, male BALB/C albino mice (29–35 g), were purchased from The National Institute of Health (NIH), Islamabad, Pakistan. Five animals were housed per group and placed in a controlled temperature and humidity-controlled room (22 °C and 66 ± 5%, respectively) in a 12 h light–dark cycle and provided with water and food ad libitum. Ethical approval was taken from the bio-ethical committee of Quaid-I-Azam University (Approval No. BEC-FBS-QAU2018-120).

The *in vivo* anti-inflammatory bioassay was performed by using the carrageenan-induced mice paw edema method. Initially, dose–response of quinazolinone-derived Mannich bases were determined and animals were first given a dose of 0.1, 1, and 10 mg/kg against 100 µL carrageenan (1% solution in normal saline)/paw. Treatment was given 60 min before carrageenan injection. Readings were taken at 4 h post carrageenan injection (Farooq et al., 2020).

The *in vivo* anti-inflammatory activity was performed following the procedure described by Koksal, *et al.* (Koksal et al., 2017) in 2017. Paw edema was induced by injecting 100 µL of 1% sterile carrageenan solution into the right hind paw of mice. Synthesized compounds (10 mg/kg), vehicle (saline with 2% DMSO) and drug (acetylsalicylic acid, ASA 10 mg/kg) were administered to the mice orally by gastric intubation 60 min before injecting carrageenan into the right hind paw. The decrease in edema was measured by vernier calipers every 2 h.

3.4. Statistical analysis

The experimental results were expressed as mean ± SD. Each test was performed in triplicate. The results were statistically analyzed by *t*-tests and ANOVA at a 95% confidence level ($p < 0.05$). GraphPad Prism software was used to calculate the lethal dose (LD_{50}) half-maximal inhibitory concentration (IC_{50}). IC_{50} is the concentration of a synthetic compound that causes 50% inhibition of the measured function. A value of $p < 0.05$ was chosen as the criterion for statistical significance.

4. Conclusions

The newly synthesized N-Mannich bases of 3, 4-dihydro-3-methyl-2(1*H*)-quinazolinone were pharmacologically evalu-

ated and their biological potential was explored by performing a series of bioassays which includes their *in silico* studies, antioxidant, enzyme inhibition, antimicrobial, cytotoxic and anti-inflammatory activities. The newly synthesized Mannich bases showed significant and encouraging results in these bioassays. All of the compounds were found to be following Lipinski's rule of five (RO5). **SH1** and **SH13** showed significant results in DPPH assay at IC_{50} of 9.94 ± 0.16 μg/mL and 11.68 ± 0.32 μg/mL, respectively. **SH7**, **SH10** and **SH13** showed good antioxidant profile in TAC and TRP bioassays. **SH3** was found to be most potent in inhibiting the α-amylase enzyme at IC_{50} of 9.48 ± 0.17 μg/mL than the standard, acarbose (13.52 ± 0.19 μg/mL). Among the library, only **SH7** was found to be effective against all bacterial strains (gram-positive and gram-negative). **SH1**, **SH7**, **SH10** and **SH12** were shortlisted from the whole library to be further testing on Hep-G2 cell lines, with the most significant results observed by **SH12** at IC_{50} of 6.48 μM at 72 h. **SH13**, substituted with acetaminophen, an analog of Paracetamol, showed significant *in vivo* anti-inflammatory activity by decreasing the paw thickness to the maximum. In a conclusion, the present study gave us the chance for further research in these areas through the hybridization of functional groups to design and develop novel bioactive compounds and to establish a rational quantitative structure–activity relationship (QSAR).

Declaration of Competing Interest

The authors declare that they have no known competing financial interests or personal relationships that could have appeared to influence the work reported in this paper.

Acknowledgments

Samra Farooq was financially supported by the Indigenous Ph.D. scholarship (PIN NO. 315-11229-2MD3-036) granted by the Higher Education Commission (HEC) of Pakistan. The authors acknowledge Prof. Carsten Bolm (RWTH Aachen University, Germany) for facilitating us with the equipment and assistant with the acquisition of characterization analysis.

Appendix A. Supplementary material

Supplementary data to this article can be found online at https://doi.org/10.1016/j.arabjc.2020.10.039.

References

Abdo, N.Y.M., Kamel, M.M., 2015. Synthesis and anticancer evaluation of 1, 3, 4-oxadiazoles, 1, 3, 4-thiadiazoles, 1, 2, 4-triazoles and Mannich bases. Chem. Pharm. Bull. 63, 369–376.

Aboraia, A.S., Abdel-Rahman, H.M., Mahfouz, N.M., El-Gendy, M. A., 2006. Novel 5-(2-hydroxyphenyl)-3-substituted-2, 3-dihydro-1, 3, 4-oxadiazole-2-thione derivatives: Promising anticancer agents. Bioorg. Med. Chem. 14, 1236–1246.

Abrão, P.H.O., Pizi, R.B., de Souza, T.B., Silva, N.C., Fregnan, A. M., Silva, F.N., Coelho, L.F.L., Malaquias, L.C.C., Dias, A.L.T., Dias, D.F., 2015. Synthesis and biological evaluation of new eugenol mannich bases as promising antifungal agents. Chem. Biol. Drug Des. 86, 459–465.

Aguilar Urbano, M., Pineda Priego, M., Prieto, P., 2013. Spectrophotometric quantitation of antioxidant capacity through the formation of a phosphomolybdenum complex: specific application to the determination of vitamin E1.

Ahn, K.S., Noh, E.J., Zhao, H.L., Jung, S.H., Kang, S.S., Kim, Y.S., 2005. Inhibition of inducible nitric oxide synthase and cyclooxygenase II by Platycodon grandiflorum saponins via suppression of nuclear factor-κB activation in RAW 264.7 cells. Life Sci. 76, 2315–2328.

Ajani, O., Audu, O., Aderohunmu, D., Owolabi, F., Olomieja, A., 2017. Review Article Undeniable Pharmacological Potentials of Quinazoline Motifs in Therapeutic Medicine. Am. J. Drug Discovery Develop. 7, 1–24.

Akhter, M., Husain, A., Azad, B., Ajmal, M., 2009. Aroylpropionic acid based 2, 5-disubstituted-1, 3, 4-oxadiazoles: Synthesis and their anti-inflammatory and analgesic activities. Eur. J. Med. Chem. 44, 2372–2378.

Akram, M., Sayeed, A., Hussain, S.Y., 2017. Synthesis and biological activities of some new heterocycles containing nitrogen and sulphur. Int. J. Pharmaceut. Sci. Res. 8, 865.

Alaa, A.-M., Abou-Zeid, L.A., ElTahir, K.E.H., Mohamed, M.A., El-Enin, M.A.A., El-Azab, A.S., 2016. Design, synthesis of 2, 3-disubstitued 4 (3H)-quinazolinone derivatives as anti-inflammatory and analgesic agents: COX-1/2 inhibitory activities and molecular docking studies. Bioorg. Med. Chem. 24, 3818–3828.

Alisi, M.A., Brufani, M., Cazzolla, N., Ceccacci, F., Dragone, P., Felici, M., Furlotti, G., Garofalo, B., La Bella, A., Lanzalunga, O., 2012. DPPH radical scavenging activity of paracetamol analogues. Tetrahedron 68, 10180–10187.

Almasirad, A., Tabatabai, S.A., Faizi, M., Kebriaeezadeh, A., Mehrabi, N., Dalvandi, A., Shafiee, A., 2004. Synthesis and anticonvulsant activity of new 2-substituted-5-[2-(2-fluorophenoxy) phenyl]-1, 3, 4-oxadiazoles and 1, 2, 4-triazoles. Bioorg. Med. Chem. Lett. 14, 6057–6059.

Almirante, L., Polo, L., Mugnaini, A., Provinciali, E., Rugarli, P., Biancotti, A., Gamba, A., Murmann, W., 1965. Derivatives of imidazole. I. Synthesis and reactions of imidazo [1, 2-α] pyridines with analgesic, antiinflammatory, antipyretic, and anticonvulsant activity. J. Med. Chem. 8, 305–312.

Al-Mulla, A., 2017. A review: biological importance of heterocyclic compounds. Der Pharma Chem. 9, 141–1472.

Al-Omary, F.A., Hassan, G.S., El-Messery, S.M., Nagi, M.N., Habib, E.-S.E., El-Subbagh, H.I., 2013. Nonclassical antifolates, part 3: synthesis, biological evaluation and molecular modeling study of some new 2-heteroarylthio-quinazolin-4-ones. Eur. J. Med. Chem. 63, 33–45.

Amanullah, M., Rehman, W., Khan, A., Akram, M., Naseer, F., 2012. Syntheses, spectral characterization and biological elucidation of some mannich bases. Asian J. Chem. 24, 5179.

Asadi, P., Khodarahmi, G., Jahanian-Najafabadi, A., Saghaie, L., Hassanzadeh, F., 2017. Biologically active heterocyclic hybrids based on quinazolinone, benzofuran and imidazolium moieties: synthesis, characterization, cytotoxic and antibacterial evaluation. Chem. Biodivers. 14, e1600411.

Ashok, M., Holla, B.S., Poojary, B., 2007. Convenient one pot synthesis and antimicrobial evaluation of some new Mannich bases carrying 4-methylthiobenzyl moiety. Eur. J. Med. Chem. 42, 1095–1101.

Banday, M.R., Mattoo, R.H., Rauf, A., 2010. Synthesis, characterization and anti-bacterial activity of 5-(alkenyl)-2-amino-and 2-(alkenyl)-5-phenyl-1, 3, 4-oxadiazoles. J. Chem. Sci. 122, 177–182.

Bayrak, H., Demirbas, A., Karaoglu, S.A., Demirbas, N., 2009. Synthesis of some new 1, 2, 4-triazoles, their Mannich and Schiff bases and evaluation of their antimicrobial activities. Eur. J. Med. Chem. 44, 1057–1066.

Bekirkan, Olcay, Ulker, Serdar, Mentese, Emre, 2015. Synthesis of some novel heterocylic compounds derived from 2-[3-(4-chlorophenyl)-5-(4-methoxybenzyl)-4H-1, 2, 4-triazol-4-yl] acetohydrazide and investigation of their lipase and α-glucosidase inhibition. Journal of enzyme inhibition and medicinal chemistry.

Belluti, F., Fontana, G., Dal Bo, L., Carenini, N., Giommarelli, C., Zunino, F., 2010. Design, synthesis and anticancer activities of stilbene-coumarin hybrid compounds: Identification of novel proapoptotic agents. Bioorg. Med. Chem. 18, 3543–3550.

Bhattacharjee, A.K., Hartell, M.G., Nichols, D.A., Hicks, R.P., Stanton, B., Van Hamont, J.E., Milhous, W.K., 2004. Structure-activity relationship study of antimalarial indolo [2, 1-b] quinazoline-6, 12-diones (tryptanthrins). Three dimensional pharmacophore modeling and identification of new antimalarial candidates. Eur. J. Med. Chem. 39, 59–67.

Birndorf, H.C., D'Alessio, J., Bagshaw, J.C., 1975. DNA-dependent RNA-polymerases from Artemia embryos: Characterization of polymerases I and II from nauplius larvae. Dev. Biol. 45, 34–43.

Bouley, R., Kumarasiri, M., Peng, Z., Otero, L.H., Song, W., Suckow, M.A., Schroeder, V.A., Wolter, W.R., Lastochkin, E., Antunes, N.T., 2015. Discovery of antibiotic (E)-3-(3-carboxyphenyl)-2-(4-cyanostyryl) quinazolin-4 (3 H)-one. J. Am. Chem. Soc. 137, 1738–1741.

Burbuliene, M.M., Jakubkiene, V., Mekuskiene, G., Udrenaite, E., Smicius, R., Vainilavicius, P., 2004. Synthesis and anti-inflammatory activity of derivatives of 5-[(2-disubstitutedamino-6-methylpyrimidin-4-yl)-sulfanylmethyl]-3H-1, 3, 4-oxadiazole-2-thiones. Il Farmaco 59, 767–774.

Carballo, J.L., Hernández-Inda, Z.L., Pérez, P., García-Grávalos, M. D., 2002. A comparison between two brine shrimp assays to detect in vitrocytotoxicity in marine natural products. BMC Biotech. 2, 17.

Cetin, A., Geçibesler, I.H., 2015. Evaluation as antioxidant agents of 1, 2, 4-triazole derivatives: effects of essential functional groups. J. Appl. Pharmaceut. Sci. 5, 120–126.

Chandra, T., Garg, N., Lata, S., Saxena, K., Kumar, A., 2010. Synthesis of substituted acridinyl pyrazoline derivatives and their evaluation for anti-inflammatory activity. Eur. J. Med. Chem. 45, 1772–1776.

Chao, S.J., Hui, X.P., Li, S., Qiu, Z.Z., Xu, P.F., Zhang, Z.Y., Wang, Q., Guan, Z.W., 2005. Synthesis and Antibacterial Activities of Novel Biphenyltetrazole Derivatives Bearing 1, 3, 4-Oxadiazole. J. Chin. Chem. Soc. 52, 539–544.

Chen, C.-J., Song, B.-A., Yang, S., Xu, G.-F., Bhadury, P.S., Jin, L.-H., Hu, D.-Y., Li, Q.-Z., Liu, F., Xue, W., 2007. Synthesis and antifungal activities of 5-(3, 4, 5-trimethoxyphenyl)-2-sulfonyl-1, 3, 4-thiadiazole and 5-(3, 4, 5-trimethoxyphenyl)-2-sulfonyl-1, 3, 4-oxadiazole derivatives. Bioorg. Med. Chem. 15, 3981–3989.

Chen, Q., Zhu, X.-L., Jiang, L.-L., Liu, Z.-M., Yang, G.-F., 2008. Synthesis, antifungal activity and CoMFA analysis of novel 1, 2, 4-triazolo [1, 5-a] pyrimidine derivatives. Eur. J. Med. Chem. 43, 595–603.

Das, S., da Silva, C.J., Silva, M.d.M., Dantas, M.D.d.A., de Fátima, Â., Ruiz, A.L.T.G., da Silva, C.M., de Carvalho, J.E., Santos, J.C., Figueiredo, I.M., 2018. Highly functionalized piperidines: Free radical scavenging, anticancer activity, DNA interaction and correlation with biological activity. J. Adv. Res. 9, 51–61.

Dewangan, D., Pandey, A., Sivakumar, T., Rajavel, R., Dubey, R.D., 2010. Synthesis of some novel 2, 5-disubstituted 1, 3, 4-oxadiazole and its analgesic, anti-inflammatory, anti-bacterial and anti-tubercular activity. Int. J. ChemTeach Res. 2, 1397–1412.

El-Gohary, N., Shaaban, M., 2014. Antimicrobial and antiquorum-sensing studies. Part 2: synthesis, antimicrobial, antiquorum-sensing and cytotoxic activities of new series of fused [1, 3, 4] thiadiazole and [1, 3] benzothiazole derivatives. Med. Chem. Res. 23, 287–299.

El-Sayed, S., Metwally, K., El-Shanawani, A.A., Abdel-Aziz, L.M., Pratsinis, H., Kletsas, D., 2017. Synthesis and anticancer activity of novel quinazolinone-based rhodanines. Chem. Cent. J. 11, 1–10.

Essghaier, B., Naouar, A., Abdelhak, J., Zid, M.F., Sadfi-Zouaoui, N., 2014. Synthesis, crystal structure and potential antimicrobial activities of di (4-sulfamoyl-phenyl-ammonium) sulphate. Microbiol. Res. 169, 504–510.

Farooq, S., Mazhar, A., Ghouri, A., Ullah, N., 2020. One-pot multicomponent synthesis and bioevaluation of tetrahydroquinoline derivatives as potential antioxidants, α-amylase enzyme inhibitors, anti-cancerous and anti-inflammatory agents. Molecules 25, 2710.

Fresno, N., Pérez-Fernández, R., Goicoechea, C., Alkorta, I., Fernández-Carvajal, A., De la Torre-Martinez, R., Quirce, S., Ferrer-Montiel, A., Martín, M.I., Goya, P., 2014. Adamantyl analogues of paracetamol as potent analgesic drugs via inhibition of TRPA1. PLoS ONE 9, e113841.

Gao, J., Radwan, M.M., León, F., Wang, X., Jacob, M.R., Tekwani, B.L., Khan, S.I., Lupien, S., Hill, R.A., Dugan, F.M., 2012. Antimicrobial and antiprotozoal activities of secondary metabolites from the fungus Eurotium repens. Med. Chem. Res. 21, 3080–3086.

Goszczyńska, A., Kwiecień, H., Fijałkowski, K., 2015. Synthesis and antibacterial activity of Schiff bases and amines derived from alkyl 2-(2-formyl-4-nitrophenoxy) alkanoates. Med. Chem. Res. 24, 3561–3577.

Grisham, M.B., Jourd'Heuil, D., Wink, D.A., 1999. I. Physiological chemistry of nitric oxide and its metabolites: implications in inflammation. Am. J. Physiol.-Gastrointestinal Liver Physiol. 276, G315–G321.

Ha, A., Ramakrishnan, E., Muthiah, R., Bhattacharjee, A., Kabilan, S., 2019. Design, synthesis, and biological evaluation of (E)-N'-((1-chloro-3, 4-dihydronaphthalen-2-yl) methylene) benzohydrazide derivatives as anti-prostate cancer agents. Front. Chem. 7, 474.

Hassanzadeh, F., Sadeghi-Aliabadi, H., Nikooei, S., Jafari, E., Vaseghi, G., 2019. Synthesis and cytotoxic evaluation of some derivatives of triazole-quinazolinone hybrids. Res. Pharmaceut. Sci. 14, 130.

Hayashi, Y., 2016. Pot economy and one-pot synthesis. Chem. Sci. 7, 866–880.

Holla, B.S., Veerendra, B., Shivananda, M., Poojary, B., 2003. Synthesis characterization and anticancer activity studies on some Mannich bases derived from 1, 2, 4-triazoles. Eur. J. Med. Chem. 38, 759–767.

Horiuchi, N., Nakagawa, K., Sasaki, Y., Minato, K., Fujiwara, Y., Nezu, K., Ohe, Y., Saijo, N., 1988. In vitro antitumor activity of mitomycin C derivative (RM-49) and new anticancer antibiotics (FK973) against lung cancer cell lines determined by tetrazolium dye (MTT) assay. Cancer Chemother. Pharmacol. 22, 246–250.

Hoskin, D.W., Ramamoorthy, A., 2008. Studies on anticancer activities of antimicrobial peptides. Biochim. Biophys. Acta (BBA)-Biomembranes 1778, 357–375.

Idhayadhulla, A., Kumar, R.S., Nasser, A.J.A., Selvin, J., Manilal, A., 2014. Synthesis of some Mannich base derivatives and their antimicrobial activity study. Arabian J. Chem. 7, 994–999.

Jayashankar, B., Rai, K.L., Baskaran, N., Sathish, H., 2009. Synthesis and pharmacological evaluation of 1, 3, 4-oxadiazole bearing bis (heterocycle) derivatives as anti-inflammatory and analgesic agents. Eur. J. Med. Chem. 44, 3898–3902.

Jin, L., Chen, J., Song, B., Chen, Z., Yang, S., Li, Q., Hu, D., Xu, R., 2006. Synthesis, structure, and bioactivity of N′-substituted benzylidene-3, 4, 5-trimethoxybenzohydrazide and 3-acetyl-2-substituted phenyl-5-(3, 4, 5-trimethoxyphenyl)-2, 3-dihydro-1, 3, 4-oxadiazole derivatives. Bioorg. Med. Chem. Lett. 16, 5036–5040.

Katircioglu, H., Beyatli, Y., Aslim, B., Yüksekdag, Z., Atici, T., 2006. Screening for antimicrobial agent production of some freshwater. Microbiology 2.

Kattappagari, K.K., Teja, C.R., Kommalapati, R.K., Poosarla, C., Gontu, S.R., Reddy, B.V.R., 2015. Role of antioxidants in facilitating the body functions: A review. J. Orofacial Sci. 7, 71.

Khan, K., Fatima, H., Taqi, M.M., Zia, M., Mirza, B., 2015. Phytochemical and in vitro biological evaluation of Artemisia scoparia Waldst. and Kit for enhanced extraction of commercially significant bioactive compounds. J. Appl. Res. Med. Aromat. Plants 2, 77–86.

Khan, S., Shin, E.M., Choi, R.J., Jung, Y.H., Kim, J., Tosun, A., Kim, Y.S., 2011. Suppression of LPS-induced inflammatory and NF-κB responses by anomalin in RAW 264.7 macrophages. J. Cell. Biochem. 112, 2179–2188.

Kim, S.D, 2004. Isolation and characterization of alpha-glucosidase inhibitor from the fungus Ganoderma lucidum. Journal of Microbiology.

Kim, J.-S., Kwon, C.-S., SoN, K.H., 2000. Inhibition of alpha-glucosidase and amylase by luteolin, a flavonoid. Biosci. Biotechnol. Biochem. 64, 2458–2461.

Koca, İ., Özgür, A., Coşkun, K.A., Tutar, Y., 2013. Synthesis and anticancer activity of acyl thioureas bearing pyrazole moiety. Bioorg. Med. Chem. 21, 3859–3865.

Kok, S.H.L., Gambari, R., Chui, C.H., Yuen, M.C.W., Lin, E., Wong, R.S.M., Lau, F.Y., Cheng, G.Y.M., Lam, W.S., Chan, S. H., 2008. Synthesis and anti-cancer activity of benzothiazole containing phthalimide on human carcinoma cell lines. Bioorg. Med. Chem. 16, 3626–3631.

Koksal, M., Ozkan-Dagliyan, I., Ozyazici, T., Kadioglu, B., Sipahi, H., Bozkurt, A., Bilge, S.S., 2017. Some novel Mannich bases of 5-(3, 4-Dichlorophenyl)-1, 3, 4-oxadiazole-2 (3H)-one and their anti-inflammatory activity. Arch. Pharm. 350, 1700153.

Krishnaraju, A.V., Rao, T.V., Sundararaju, D., Vanisree, M., Tsay, H.-S., Subbaraju, G.V., 2005. Assessment of bioactivity of Indian medicinal plants using brine shrimp (Artemia salina) lethality assay. Int. J. Appl. Sci. Eng. 3, 125–134.

Kumar, A., Tyagi, M., Srivastava, V., 2003. Newer potential quinazolinones as hypotensive agents.

Kumar, N.S., Pradeep, T., Jani, G., Silpa, D., Kumar, B.V., 2012. Design, synthesis, and antimicrobial screening of novel pyridyl-2-amidrazone incorporated isatin mannich bases. J. Adv. Pharm. Technol. Res. 3, 57.

Liu, B., Gao, H.M., Wang, J.Y., Jeohn, G.H., Cooper, C.L., Hong, J. S., 2002. Role of nitric oxide in inflammation-mediated neurodegeneration. Ann. New York Acad. Sci. 962, 318–331.

Lobo, V., Patil, A., Phatak, A., Chandra, N., 2010. Free radicals, antioxidants and functional foods: Impact on human health. Pharmacogn. Rev. 4, 118.

Lyons, C.R., 1995. The role of nitric oxide in inflammation. In: Advances in Immunology, Elsevier, pp. 323–371.

Marzaro, G., Guiotto, A., Chilin, A., 2012. Quinazoline derivatives as potential anticancer agents: a patent review (2007–2010). Expert Opin. Ther. Pat. 22, 223–252.

McLaughlin, J., 1982. Brine shrimp: a convenient general bioassay for active constituents. Planta med 45, 31–32.

Medley, J.W., Movassaghi, M., 2013. Robinson's landmark synthesis of tropinone. Chem. Commun. 49, 10775–10777.

Mistry, B., Patel, R.V., Keum, Y.-S., Kim, D.H., 2017. Synthesis of N-Mannich bases of berberine linking piperazine moieties revealing anticancer and antioxidant effects. Saudi J. Biol. Sci. 24, 36–44.

Mital, A., 2007. Recent advances in antimalarial compounds and their patents. Curr. Med. Chem. 14, 759–773.

Moncada, S., 1997. Nitric oxide in the vasculature: physiology and pathophysiology. Ann. N. Y. Acad. Sci. 811, 60–69.

Murad, F., 1998. Nitric oxide signaling: would you believe that a simple free radical could be a second messenger, autacoid, paracrine substance, neurotransmitter, and hormone?. Recent Prog. Horm. Res. 53, 43.

Nanjunda, S., Swamy, S., Basppa, P.B., Prabhuswamy, B., Doreswamy, B., 2006. Crystal structure of novel 2-butyl-4-chloro-1HImidazolyl-5-carboxaldehyde. Eur. J. Med. Chem. 41, 531-538.533.

Nishiyama, T., Sakita, K., Fuchigami, T., Fukui, T., 1998. Antioxidant activities of fused heterocyclic compounds, xanthene-2, 7-diols with BHT or catechol skeleton. Polym. Degrad. Stab. 62, 529–534.

Nishiyama, T., Hashiguchi, Y., Sakata, T., Sakaguchi, T., 2003. Antioxidant activity of the fused heterocyclic compounds, 1, 2, 3, 4-tetrahydroquinolines, and related compounds—effect of ortho-substituents. Polym. Degrad. Stab. 79, 225–230.

Padmaja, A., Payani, T., Reddy, G.D., Padmavathi, V., 2009. Synthesis, antimicrobial and antioxidant activities of substituted pyrazoles, isoxazoles, pyrimidine and thioxopyrimidine derivatives. Eur. J. Med. Chem. 44, 4557–4566.

Pandeya, S., Sriram, D., Nath, G., De Clercq, E., 1999. Synthesis and antimicrobial activity of Schiff and Mannich bases of isatin and its derivatives with pyrimidine. Il Farmaco 54, 624–628.

Peng, L.-P., Nagarajan, S., Rasheed, S., Zhou, C.-H., 2015. Synthesis and biological evaluation of a new class of quinazolinone azoles as potential antimicrobial agents and their interactions with calf thymus DNA and human serum albumin. Medicinal Chem. Commun. 6, 222–229.

Poorirani, S., Sadeghian-Rizi, S., Khodarahmi, G., Khajouei, M.R., Hassanzadeh, F., 2018. Synthesis and cytotoxic evaluation of novel quinazolinone derivatives as potential anticancer agents. Res. Pharmaceut. Sci. 13, 450.

Prieto, P., Pineda, M., Aguilar, M., 1999. Spectrophotometric quantitation of antioxidant capacity through the formation of a phosphomolybdenum complex: specific application to the determination of vitamin E. Anal. Biochem. 269, 337–341.

Raghavendra, N.M., Thampi, P., Gurubasavarajaswamy, P.M., Sriram, D., 2007. Synthesis, Antitubercular and Anticancer Activities of Substituted Furyl-quinazolin-3 (4H)-ones. Archiv der pharmazie: Int. J. Pharmaceut. Medicinal Chem. 340, 635–641.

Raghunandan, D., Ravishankar, B., Sharanbasava, G., Mahesh, D. B., Harsoor, V., Yalagatti, M.S., Bhagawanraju, M., Venkataraman, A., 2011. Anti-cancer studies of noble metal nanoparticles synthesized using different plant extracts. Cancer Nanotechnol. 2, 57–65.

Rakesh, K., Manukumar, H., Gowda, D.C., 2015. Schiff's bases of quinazolinone derivatives: synthesis and SAR studies of a novel series of potential anti-inflammatory and antioxidants. Bioorg. Med. Chem. Lett. 25, 1072–1077.

Rk, M., Begum, S., Begum, A., 2018. Antioxidant potential of piperidine containing compounds-a short review. Atherosclerosis 10, 12.

Roy, P.J., Landry, K., Leblanc, Y., Chun, L., Tsou, N., 1997. Condensation of 2-amino-5-chlorobenzoxazole with α-bromoketones: a mechanistic study. Heterocycles 11, 2239–2246.

Rubat, C., Coudert, P., Albuisson, E., Bastide, J., Couquelet, J., Tronche, P., 1992. Synthesis of Mannich bases of arylidenepyridazinones as analgesic agents. J. Pharm. Sci. 81, 1084–1087.

Ryu, C.-K., Kim, Y.H., Im, H.A., Kim, J.Y., Yoon, J.H., Kim, A., 2012. Synthesis and antifungal activity of 6, 7-bis (arylthio)-quinazoline-5, 8-diones and furo [2, 3-f] quinazolin-5-ols. Bioorg. Med. Chem. Lett. 22, 500–503.

Saad, H.,1996. Design synthesis, characterization and antibacterial activity of 1, 3, 4-Oxadiazolederivatives. Indian J. Chem. B 35, 980–982.

Saini, M.S., Kumar, A., Dwivedi, J., Singh, R., 2013. A review: biological significances of heterocyclic compounds. Int. J. Pharmaceut. Sci. Res. 4, 66–77.

Saleh, S.S., AL-Salihi, S.S., Mohammed, I.A., 2019. Biological activity Study for some heterocyclic compounds and their impact on the gram positive and negative bacteria. Energy Procedia 157, 296–306.

Samu, G.F., Janáky, C., 2017. Tailoring the interfaces in conducting polymer composites by controlled polymerization. In: Hybrid polymer composite materials, Elsevier, pp. 101–134.

Sanchez, C., Gupta, M., Vasquez, M., De Noriega, Y., Montenegro, G., 1993. Bioessay with brine Artemia to predict antibacterial and pharmacologic activity. Rev. Med. Panama 18, 62–69.

Santos-Sánchez, N.F., Salas-Coronado, R., Villanueva-Cañongo, C., Hernández-Carlos, B., 2019. Antioxidant compounds and their antioxidant mechanism. In: Antioxidants, IntechOpen.

Senthilraja, P., Kathiresan, K., 2015. In vitro cytotoxicity MTT assay in Vero, HepG2 and MCF-7 cell lines study of Marine Yeast. J. Appl. Pharmaceut. Sci. 5, 80–84.

Sharma, P.C., Kaur, G., Pahwa, R., Sharma, A., Rajak, H., 2011. Quinazolinone analogs as potential therapeutic agents. Curr. Med. Chem. 18, 4786–4812.

Shi, L.-P., Jiang, K.-M., Jiang, J.-J., Jin, Y., Tao, Y.-H., Li, K., Wang, X.-H., Lin, J., 2013. Synthesis and antimicrobial activity of polyhalobenzonitrile quinazolin-4 (3H)-one derivatives. Bioorg. Med. Chem. Lett. 23, 5958–5963.

Shyma, P., Kalluraya, B., Peethambar, S., Vijesh, A., 2015. Synthesis, characterization, antidiabetic and antioxidant activity of 1, 3, 4-oxadiazole derivatives bearing 6-methyl pyridine moiety. Der Pharma Chem. 7, 137–145.

Siegel, R.L., Miller, K.D., Jemal, A., 2016. Cancer statistics, 2016, CA: A Cancer J. Clinicians 66, 7–30.

Simmons, D.L., Wagner, D., Westover, K., 2000. Nonsteroidal anti-inflammatory drugs, acetaminophen, cyclooxygenase 2, and fever. Clin. Infect. Dis. 31, S211–S218.

Sivakumar, K.K., Rajasekaran, A., Senthilkumar, P., Wattamwar, P. P., 2014. Conventional and microwave assisted synthesis of pyrazolone Mannich bases possessing anti-inflammatory, analgesic, ulcerogenic effect and antimicrobial properties. Bioorg. Med. Chem. Lett. 24, 2940–2944.

SwissADME Software. Available online: in, 2020.

Solis, P.N., Wright, C.W., Anderson, M.M., Gupta, M.P., Phillipson, J.D., 1993. A microwell cytotoxicity assay using Artemia salina (brine shrimp). Planta Med. 59, 250–252.

Sridhar, S.K., Pandeya, S.N., Stables, J.P., Ramesh, A., 2002. Anticonvulsant activity of hydrazones, Schiff and Mannich bases of isatin derivatives. Eur. J. Pharmaceut. Sci. 16, 129–132.

Srinivas, K., Srinivas, U., Bhanuprakash, K., Harakishore, K., Murthy, U., Rao, V.J., 2006. Synthesis and antibacterial activity of various substituted s-triazines. Eur. J. Med. Chem. 41, 1240–1246.

Sydnes, M.O., 2014. One-pot reactions: A step towards greener chemistry. Curr. Green Chem. 1, 216–226.

Tai, Z., Cai, L., Dai, L., Dong, L., Wang, M., Yang, Y., Cao, Q., Ding, Z., 2011. Antioxidant activity and chemical constituents of edible flower of Sophora viciifolia. Food Chem. 126, 1648–1654.

Taj, T., Kamble, R.R., Gireesh, T., Hunnur, R.K., Margankop, S.B., 2011. One-pot synthesis of pyrazoline derivatised carbazoles as antitubercular, anticancer agents, their DNA cleavage and antioxidant activities. Eur. J. Med. Chem. 46, 4366–4373.

Tanabe, Y., Kawai, A., Yoshida, Y., Ogura, M., Okumura, H., 1997. Preparation of fused thiadiazolo-and imidazo-benzothiazoles from 2-aminobenzothiazoles. Their fungicidal activity. Heterocycles 8, 1579–1588.

Tramontini, M., 1973. " Advances in the chemistry of mannich bases. Amino Acids 1, 1.

Trapani, G., Franco, M., Latrofa, A., Genchi, G., Liso, G., 1992. Synthesis and benzodiazepine receptor binding of some 4H-pyrimido [2, 1-b] benzothiazol-4-ones. Eur. J. Med. Chem. 27, 39–44.

Ünver, Y., Deniz, S., Çelik, F., Akar, Z., Küçük, M., Sancak, K., 2016. Synthesis of new 1, 2, 4-triazole compounds containing Schiff and Mannich bases (morpholine) with antioxidant and antimicrobial activities. J. Enzyme Inhib. Med. Chem. 31, 89–95.

Valko, M., Leibfritz, D., Moncol, J., Cronin, M.T., Mazur, M., Telser, J., 2007. Free radicals and antioxidants in normal physiological functions and human disease. Int. J. Biochem. Cell Biol. 39, 44–84.

Wade, J.J., Hegel, R.F., Toso, C.B., 1979. Reaction of 2-aminobenzazoles with dimethyl 2-aminofumarate. Synthesis and nuclear magnetic resonance spectroscopy of 4-oxopyrimido [2, 1-b] benzazoles. J. Organ. Chem. 44, 1811–1816.

Wang, M., Gao, M., Mock, B.H., Miller, K.D., Sledge, G.W., Hutchins, G.D., Zheng, Q.-H., 2006. Synthesis of carbon-11 labeled fluorinated 2-arylbenzothiazoles as novel potential PET cancer imaging agents. Bioorg. Med. Chem. 14, 8599–8607.

Wang, Z., Wang, M., Yao, X., Li, Y., Tan, J., Wang, L., Qiao, W., Geng, Y., Liu, Y., Wang, Q., 2012. Design, synthesis and antiviral activity of novel quinazolinones. Eur. J. Med. Chem. 53, 275–282.

Wiji Prasetyaningrum, P., Bahtiar, A., Hayun, H., 2018. Synthesis and cytotoxicity evaluation of novel asymmetrical mono-carbonyl analogs of curcumin (AMACs) against Vero, HeLa, and MCF7 Cell Lines. Scientia Pharmaceut. 86, 25.

Yehye, W.A., Abdul Rahman, N., Alhadi, A.A., Khaledi, H., Ng, S. W., Ariffin, A., 2012. Butylated hydroxytoluene analogs: Synthesis and evaluation of their multipotent antioxidant activities. Molecules 17, 7645–7665.

Zarghi, A., Tabatabai, S.A., Faizi, M., Ahadian, A., Navabi, P., Zanganeh, V., Shafiee, A., 2005. Synthesis and anticonvulsant activity of new 2-substituted-5-(2-benzyloxyphenyl)-1, 3, 4-oxadiazoles. Bioorg. Med. Chem. Lett. 15, 1863–1865.

Zarghi, A., Hamedi, S., Tootooni, F., Amini, B., Sharifi, B., Faizi, M., Tabatabai, S.A., Shafiee, A., 2008. Synthesis and pharmacological evaluation of new 2-substituted-5-{2-[(2-halobenzyl) thio) phenyl}-1, 3, 4-oxadiazoles as anticonvulsant agents. Sci. Pharm. 76, 185–202.

Zhang, Y., Zhou, J., Zhang, H., 2010. Use of 8-quinolinol and its analogs to target cancer stem cells, in, Google patents.